Table of contents:

Abstract:

Solar electricity is seen as being a significant source of renewable energy. The photovoltaic generator is a source characterized by only one point of operation where the generated power is maximum called maximum power point(MPP). Unfortunately that point moves according to the weather conditions (temperature and irradiance) and needs a controller to track it. Many MPPT techniques were proposed such as perturb and observe (P&O), Incremental conductance (InC), the fractional open circuit voltage (FOCV) ,fractional short circuit current (FSCC)

This work presents an improved sun tracker controller for PV systems. An improved P&O algorithm using a microcontroller to achieve this objective. The developed MPPT uses the Sun tracker to extract the maximum power.

The simulation results show that the response of the proposed design is faster than the P&O algorithm without sun tracker.

General introduction:

The continuous increase of the world energy demand, and the increasing concerns about global warming and the damage to the environment because of the use of the conventional energy resources (oil and its derivatives), motivate the governments and organizations to seek and make investments in alternative renewable energy resources (wind, geothermal, sea waves and solar energy).

Among those alternative resources, PV generation comes as a favorite choice in Algeria, due to its distinctive advantages such as the simplicity of installation, the low cost of maintenance. In addition to its abundance especially in North Africa Sahara region where our country is known to be most exposed region with an annual average of 3500 hours of sunshine per year [1].

Although all these latter mentioned advantages, PV generation suffers mainly from two main drawbacks, its high dependence to the weather conditions (temperature and irradiance) and its relatively low conversion efficiency that varies from 12% to 29% for very expensive units. The PV generation plant efficiency is mainly affected by three factors, the efficiency of the PV panel, the efficiency of the power electronic converter and the efficiency of the maximum power point tracking (MPPT) algorithm which needs to be increased as higher as possible. And it is the cheapest among the others.

MPPT algorithms are necessary due to the fact that the PV arrays have a nonlinear voltage-current characteristic curve with a unique maximum power point that needs to be continuously tracked as the weather conditions change. In the past few years, several MPPT algorithms have been proposed such as perturb and observe (P&O), Incremental conductance (InC), the fractional open circuit voltage (FOCV) ,fractional short circuit current (FSCC).

The first chapter deals with the PV panel modeling and operating principles. The second one is devoted to the power electronic circuits and power transfer control in photovoltaic system.

Thirdly, the different MPPT algorithm techniques are presented. Finally, the design and simulation of a sun Tracking System with MPPT is performed using the ISIS PROTEUS software package.

1.1 Introduction:

The photovoltaic is the field of research and technology related to the application of solar cells to convert solar energy into electricity. The term “photo” means light and “voltaic” means electricity.

Although the PV effect was firstly observed by French scientist Edmund Bacquirel in 1839, it was not fully understood until the development of quantum theory of light and solid state physics in the middle of the twenty century. With the discover made by the Albert Einstein “the photoelectric effect”, the ability of some semiconductor materials to convert electromagnetic radiations directly into electrical current were explained.

1.2 The operation principle of photovoltaic cell:

The solar cell is the elementary block for the PV panels, most are made from silicon even though there’re other materials such as GaAs(Gallium Arsenide), CdTe (Cadmium Telluride) and CIS(Copper Indium Diselenide $CuInSe_2$)[2],which vary from each other in terms of light absorption efficiency, energy conversion efficiency and the manufacturing technology.

Basically, the solar cell is a p-n junction, made from two different doped silicon layers, a p-type layer (doped with an acceptor element impurity like Boron B to form free holes) and an n-type layer(doped with a donor element impurity like Phosphorus P to form free electrons), when the two layers are brought in contact, the free electrons of the n-layer are diffused in the p-side, similarly the free holes in the p-layer are diffused in the n-side. This creates an internal electric field between the two sides that is a potential barrier and we can say that the equilibrium is reached.

When the photon of the solar radiation with an energy level above the material band gap strikes the solar cell, it creates an electron-hole pair, these pairs is generated at both sides of the p-n junction. The minority carriers (electrons in the p-side and holes in the n-side) are defused to the junction and swept away in the opposite direction (electrons to the n-side and holes to p-side) by the electric field, generating a current in the cell, this may be further illustrated by the figure-2.1-.

Metallic contacts are added at both sides to collect the electrons and holes and the current can flow. But in the case of the n-type layer which faces the sun light the contacts are made as strips to allow the solar light to pass and they are called fingers.

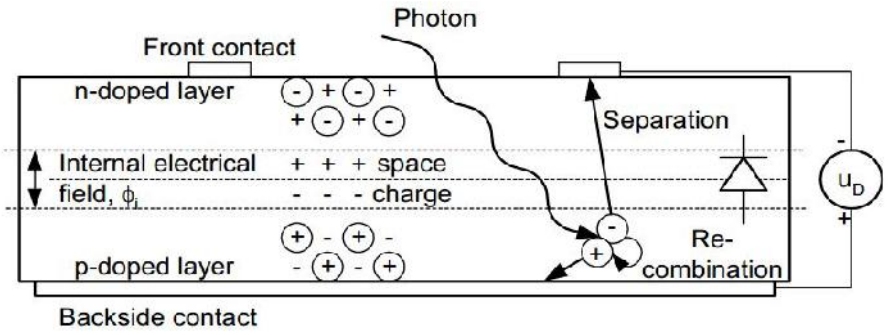

Fig-1.1-: Cross section of the PN junction and processes occurred at the irradiated PV cell [3].

1.3 PV cell modelling

As the solar cell shows a nonlinear (I-V) characteristic curve, many models for the equivalent circuit were suggested in the aim of explaining this nonlinear behaviour (Single-diode model, Double-diode model and the simplified model [4]).

The single-diode model with its two versions (depending of the shunt resistance, if it's taken in consideration or not) as shown in the two below figures, is the most used model in PV cell simulation as they offer a good compromise between complexity and the quality of the gotten results compared to the real ones.

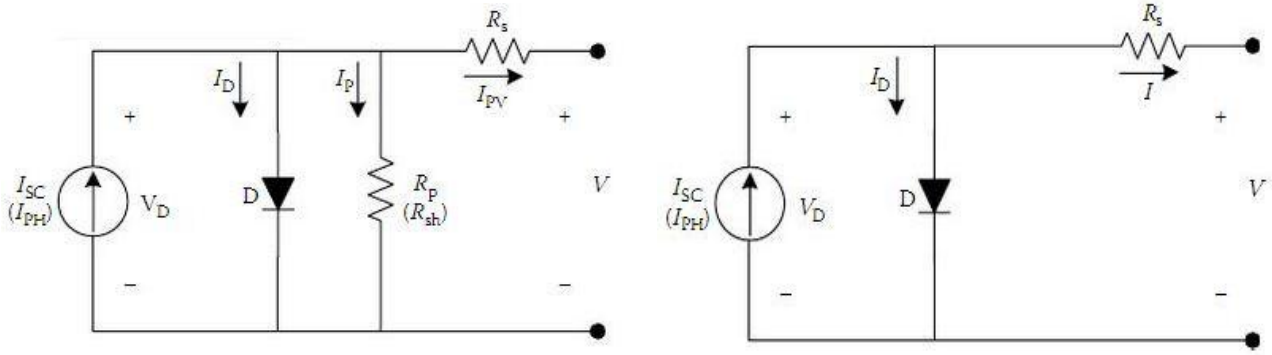

Fig-1.2-: The single-diode model of solar cell [3].

And the following analysis can be done based on the equivalent circuit of figure (1.2):

$$I=I_{PH}-I_D-I_{SH} \qquad (1.1)$$

Where:

I_{PH} : is the light or the photo current, and it depends on the irradiance and the temperature, it can be measured at some reference conditions as written in the (1.2):

$$I_{PH}=\frac{G}{G_{ref}}I_{SC,ref}+K_I(T_C+T_{Cref}) \qquad (1.2)$$

Where: G, G_{ref}: the actual and reference irradiance conditions (W/m^2).

K_I: the temperature coefficient of short-circuit current (A/°K).

T_C,T_{Cref}:the actual and reference temperature conditions (°K).

I_D: is the diode current, and it can be expressed as follows [3]:

$$I_D=I_0[\exp\left(\frac{q(V+RS*I)}{AKT_C}\right)-1] \qquad (1.3)$$

Where: q: the electron charge 1.069×10^{-19} C.

K: Boltzman constant 1.381×10^{-23} J/K.

A: the ideality factor of the diode (1<a<2).

R_S: the series resistance (Ω).

I_0: the reverse diode saturation current and it's a function of (T) [3]:

$$I_0=I_{0,REF}(\frac{T_C}{T_{CREF}})^3\exp[(\frac{q\,E_g}{K\,A})(\frac{1}{T_{C,REF}}-\frac{1}{T_C})] \qquad (1.4)$$

Where: E_G: material band-gap energy (1.12 eV for Silicon).

$$I_{0ref}=\frac{I_{SC,ref}}{\exp\left(\frac{qV_{OCref}}{AKT_C}\right)-1} \qquad (1.5)$$

I_{SH}: is the current flowing in the shunt resistance branch and its expression

Is the following [3]:

$$I_{SH}=\frac{V-IR_S}{R_{SH}} \qquad (1.6)$$

So the equation (1.1) can written in more details after substituting (1.2),(1.3) and(1.6) [3]:

$$I=\frac{G}{G_{ref}}I_{SC,ref}+K_I\left(T_C+T_{Cref}\right)-I_0\left[\exp\left(\frac{q(V+RS*I)}{AKT_C}\right)-1\right]-\frac{V-IR_S}{R_{SH}} \qquad (1.7)$$

1.4 Matlab /Similink model:

The model was developed in the Matlab/Similink environment as shown in fig-1.3-and it is implemented using single-diode model.

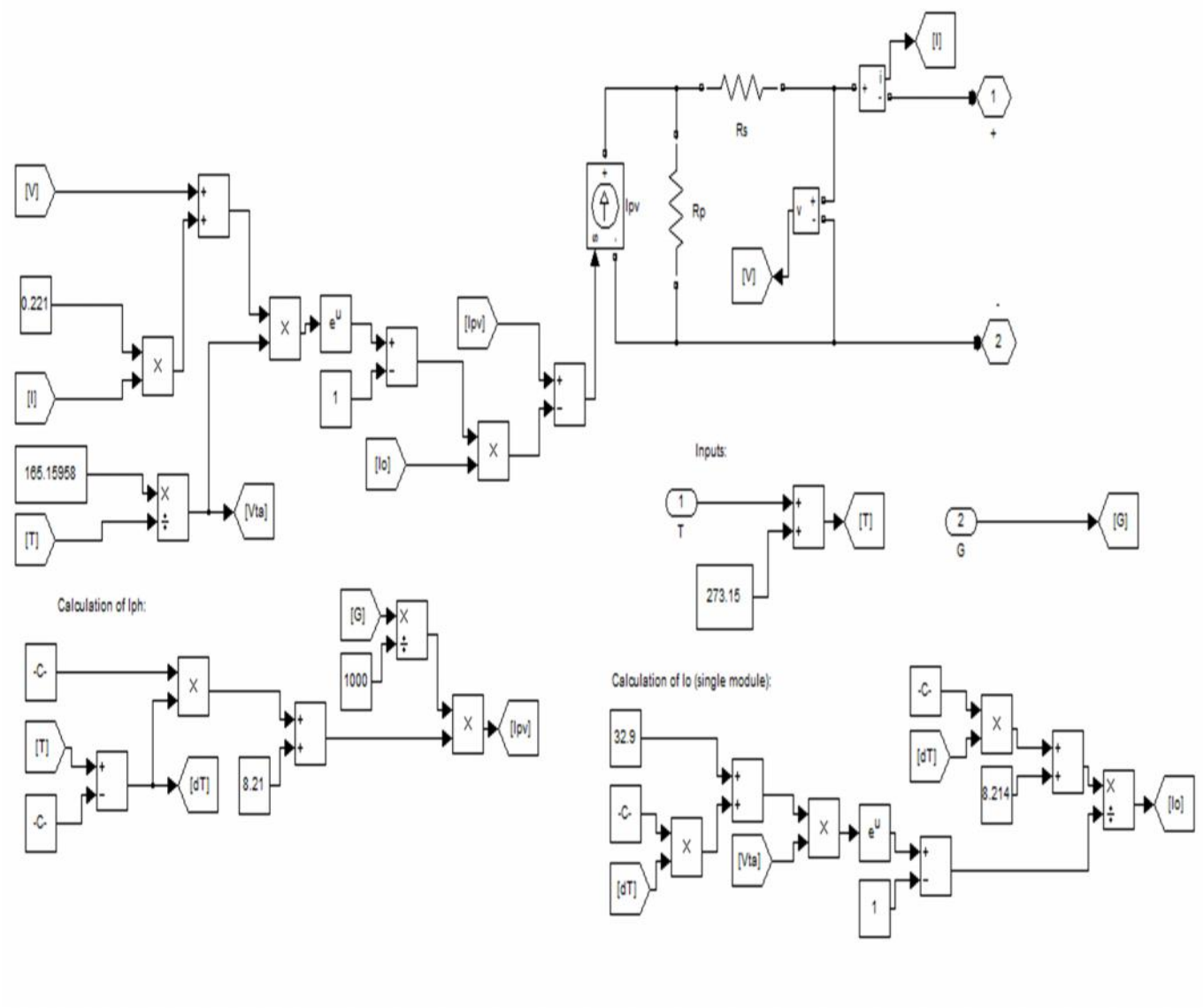

Fig-1.3-: The Matlab/Similink Model of the PV module.

1.5 The model simulation results:

The application of different irradiance and temperature conditions applied to the designed model is shown in figure(1.4). The parameters of the KC200GT solar module were used to run the implemented model .

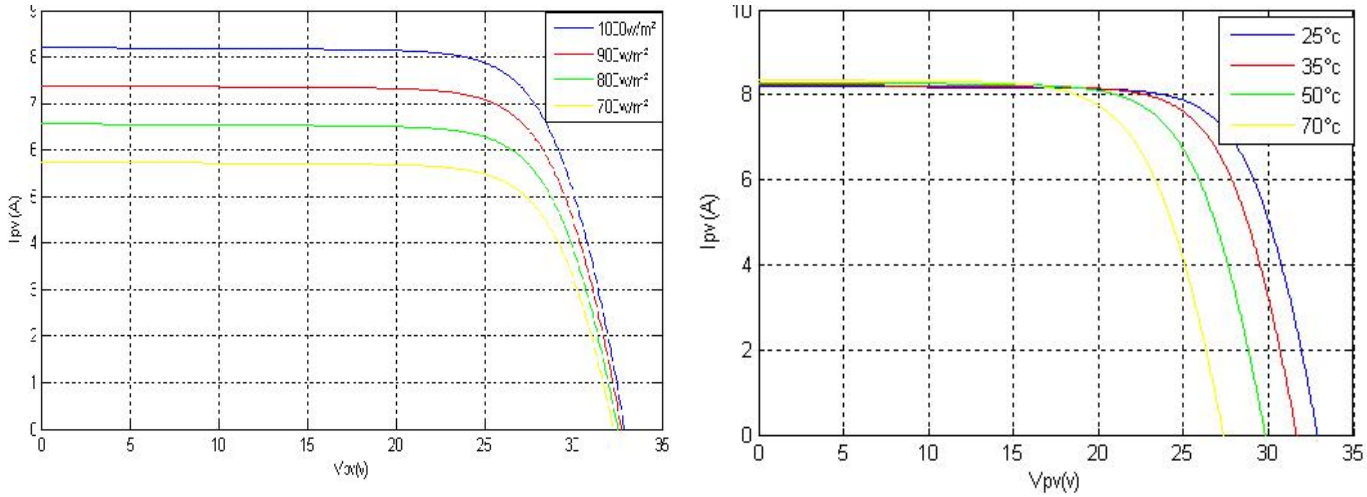

Fig-1.4-: The I-V characteristic curve of the PV module at different irradiance and temperature conditions.

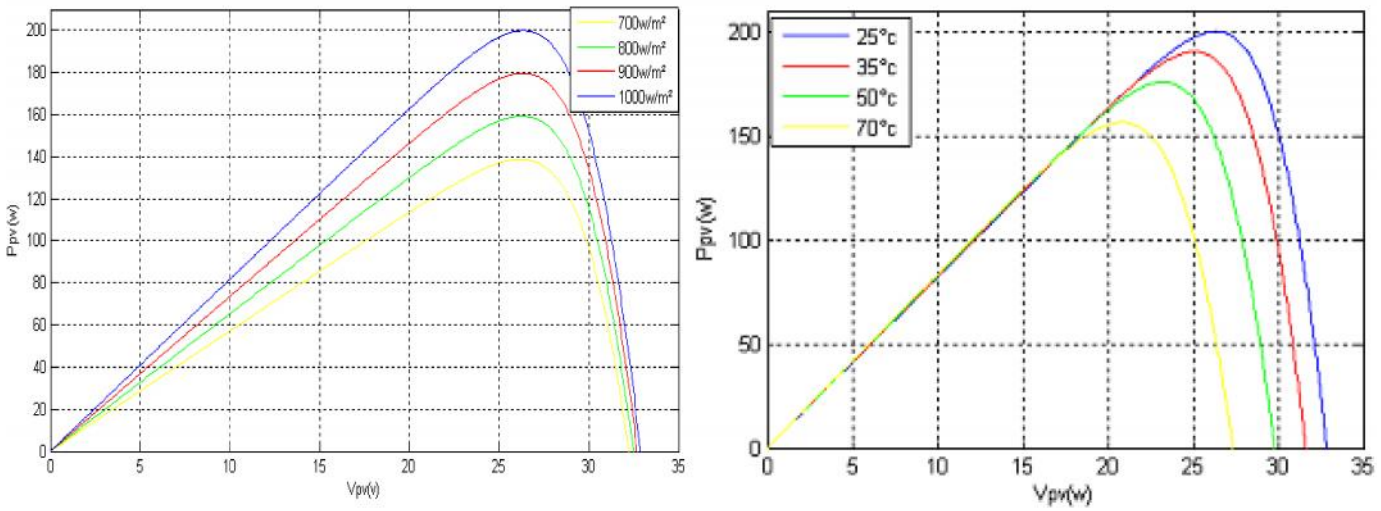

Fig-1.5-: The P-V characteristic curve of the PV module at different irradiance and temperature conditions.

1.6 Observations and comments:

From the previous plots, one can see short circuit current test of the cell that is highly affected by the illumination level, while the effect of this latter is relatively weak on the open circuit voltage test. Regarding the maximum power output of the cell, it is clear that when the irradiance is higher the cell generates more power.

The temperature on the other hand, affects mostly the open circuit voltage while the short circuit current remains constant and the output power is reduced significantly at high degrees due to the dependency of the V_{OC} on the temperature.

1.7 Conclusion:

In this chapter, a Matlab/Similink model was developed based on the single-diode model, and the resulting waveforms were checked referring to the data sheet provided by the manufacturer.

A non linear characteristic curve is describing the panel current-voltage I-V, with a unique maximum power point (MPP) which needs to be tracked to ensure that the maximum power is being absorbed from the PV panel. This task is entrusted to the maximum power point tracking algorithms (MPPT) that are later discussed in depth in dedicated chapter.

2.1 Introduction:

The purpose of this chapter is to cover the power electronic circuits in photovoltaic system, basically the following functions were performed: DC/DC and DC/AC conversion.

We will select the components values used in our system. And the constructed circuit will be simulated in Simulink to see the curves of different parameters.

2.2 DC-DC Converters:

In this section different DC/DC converter circuits were discussed and the principles of power conversion switching were introduced. The DC/DC converters can have two distinct modes of operation: Continuous Conduction Mode (CCM) and Discontinuous Conduction Mode (DCM). In practice, a converter may operate in both modes, which have significantly different characteristics. Therefore, a converter and its control should be designed based on both modes of operation. However, in this project, the DC/DC converters operated in CCM is considered.

The three basic DC/DC converters use a pair of switches, usually one controlled and one uncontrolled (i.e. diode), to achieve unidirectional power flow from input to output, and also consists of capacitors, inductors and switches. All these devices ideally do not consume any power, which is the reason for the high efficiencies of switching converters. The switch is realized with a switched mode semiconductor device (usually a MOSFET). If the semiconductor device is in the off-state, its current is zero and hence its power dissipation is zero. If the device is in the on-state (i.e. saturated), the voltage drop across it will be close to zero and hence the dissipated power will be very small. During the operation of the converter, the switch will be switched at a constant frequency f_s with an on-time of DT_s, and an off-time of $(1 - D)T_s$, where T_s is the switching period $T_s = 1/f_s$ and D is the duty cycle of the switch ($D \in [0, 1]$) and $D=T_{on}/(T_{on} + T_{off})$.

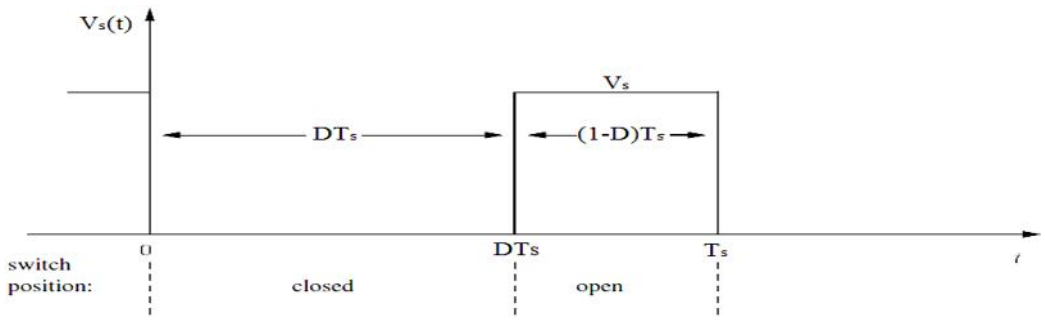

Fig-2.1-: The voltage across the switch in a period.

In the analysis of the three DC-DC converters topologies we assumed made that the operation of each converter is as follows:

- The circuit is operating in the steady state
- The circuit is operating in the CCM
- The capacitor is large enough to assume a constant output voltage
- The component are ideal.

2.2.1 Buck (step-down) converter:

The basic circuit configuration used in the buck converter is shown in Figure-2.2. As you can see there are only four main components: switching power MOSFET Q, Schottky diode D, inductor L and output capacitor C (The capacitor and inductor to store and transfer energy from input to output. They also filter or smooth voltage and current output).

Circuit Operation: When the switch is ON for a time duration DT, the switch conducts the inductor current and the diode becomes reverse biased. This results in a positive voltage $v_L = V_g - V_o$ across the inductor. This voltage causes a linear increase in the inductor current i_L. When the switch is turned OFF, because of the inductive energy storage, i_L continues to flow. This current now flows through the diode, and $v_L = -V_o$ for a time duration (1-D)T until the switch is turned ON again.

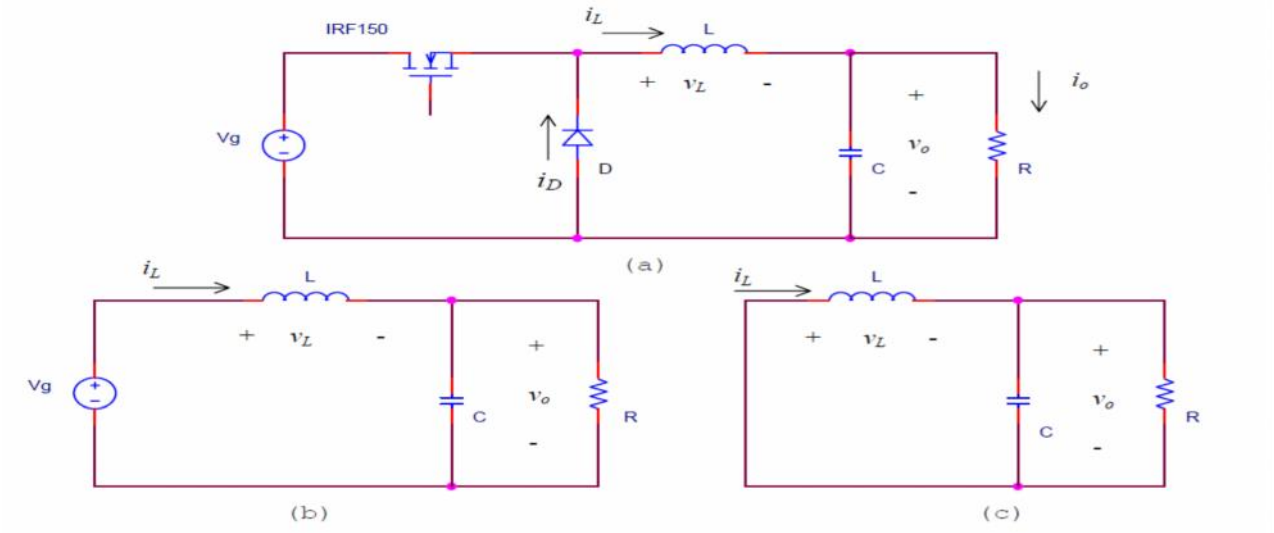

Fig-2.2-: (a) Buck converter circuit diagram

(b) Switch ON for a time duration DT (c) Switch OFF for time duration (1-D) T. [6]

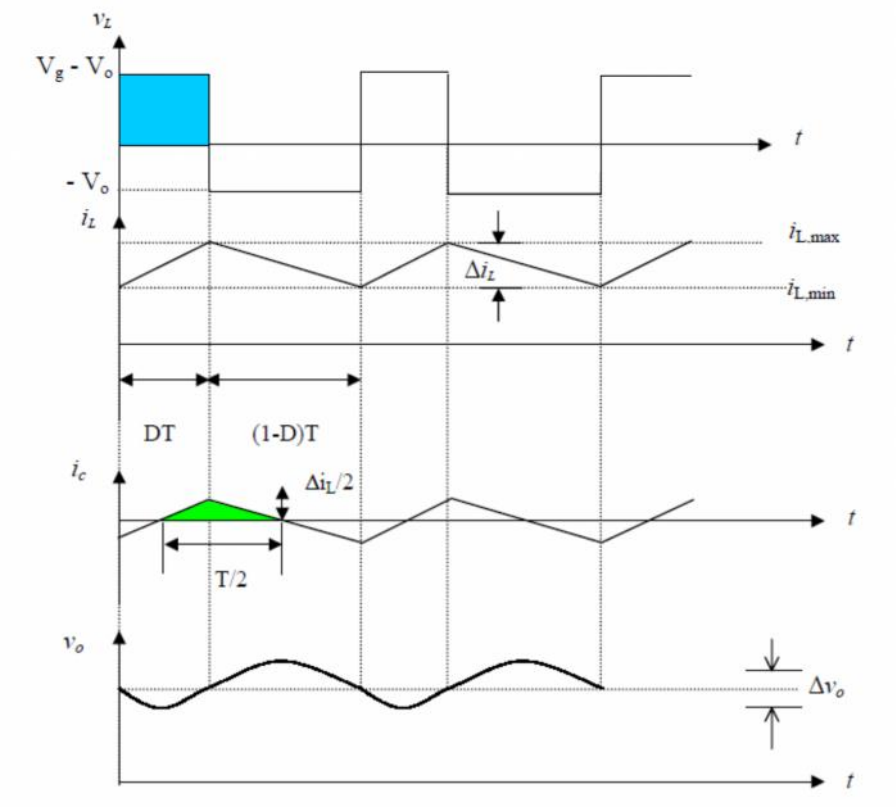

Fig-2.3-: Current and voltage waveforms in the buck converter. [6]

Equating the integral of the inductor voltage over one time period to zero yields:

$$\int_0^T v_L(t)dt = \int_0^{Ton} v_L(t)dt + \int_0^{Toff} v_L(t)dt = 0 \qquad (2.1)$$

$$V_L = DT(V_g - V_o) + (1 - D)T(-V_o) = 0 \Rightarrow V_o = D \cdot V_g \qquad (2.2)$$

The conversion ratio can be determined to be:

$$M(D) = \frac{V_o}{V_g} = D \qquad (2.3)$$

2.2.2 Boost (step-up) converter:

The basic boost converter is no more complicated than the buck converter, but has the components arranged. A boost converter is simply is a particular type of power converter with an output DC voltage greater than the input DC voltage. This type of circuit is used to step-up a source voltage to a higher, regulated voltage, allowing one power supply to provide different driving voltages.

Circuit Operation: When the switch is ON for a time duration DT, the switch conducts the inductor current and the diode becomes reverse biased. This results in a positive voltage $v_L = V_g$ across the inductor. This voltage causes a linear increase in the inductor current i_L. When the switch is turned OFF, because of the inductive energy storage, i_L continues to flow. This current now flows through the diode, and $v_L = V_g - V_o$ for a time duration (1-D)T until the switch is turned ON again.

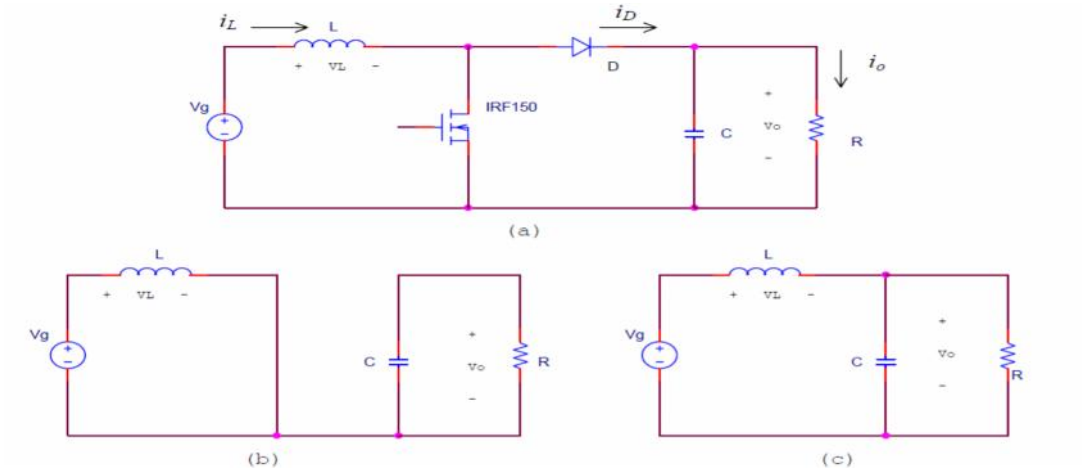

Fig-2.4-:(a) Boost converter circuit diagram

(b) Switch ON for a time duration DT (c) Switch OFF for a time duration (1-D)T. [6]

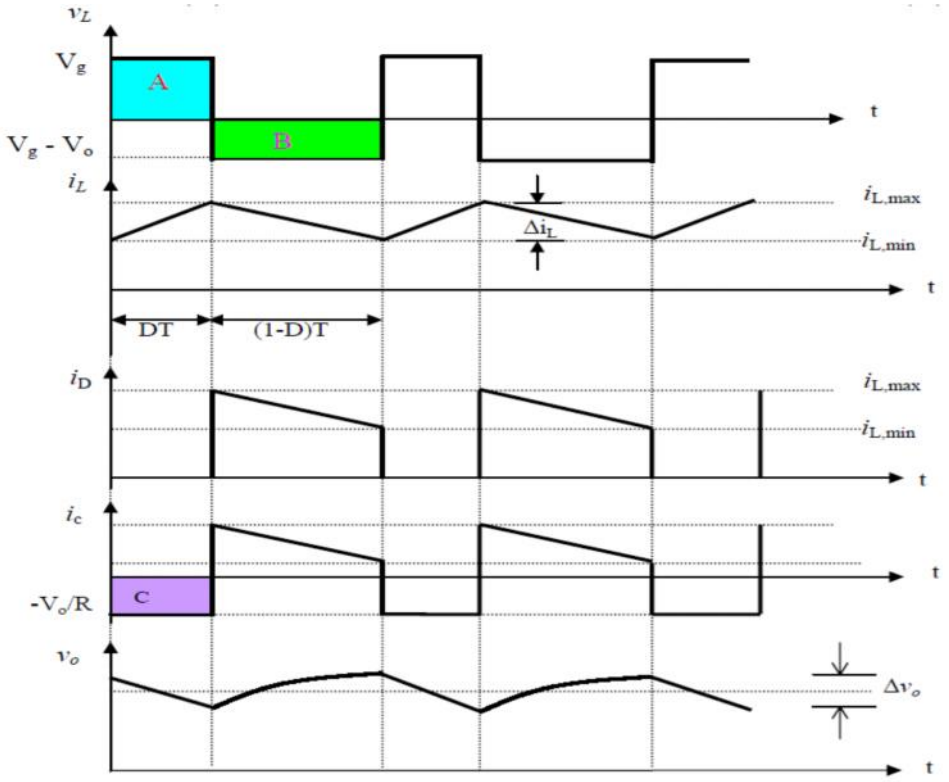

Fig-2.5-: Current and voltage waveforms in the boost converter. [6]

Equating the integral of the inductor voltage over one time period to zero yields

$$\int_0^T v_L(t)dt = \int_0^{Ton} v_L(t)dt + \int_0^{Toff} v_L(t)dt = 0 \quad (2.4)$$

$$V_L = DT\,V_g + (1-D)T(V_g - V_o) = 0 \Rightarrow V_o = \frac{1}{1-D}\,V_g \quad (2.5)$$

The conversion ratio can be determined to be:

$$M(D) = \frac{V_o}{V_g} = \frac{1}{1-D} \quad (2.6)$$

2.2.3 Buck-boost converter: [6]

The main components in a buck-boost converter are again much the same as in the buck and boost types, but they reconfigured in a different way again Figure-2.6.

Circuit Operation: When the switch is ON for a time duration DT, the switch conducts the inductor current and the diode becomes reverse biased. This results in a positive voltage $v_L = V_g$ across the inductor. This voltage causes a linear increase in the inductor current i_L. When the switch is turned OFF, because of the inductive energy storage, i_L continues to flow. This current now flows through the diode, and $v_L = -V_o$ for a time duration (1-D)T until the switch is turned ON again.

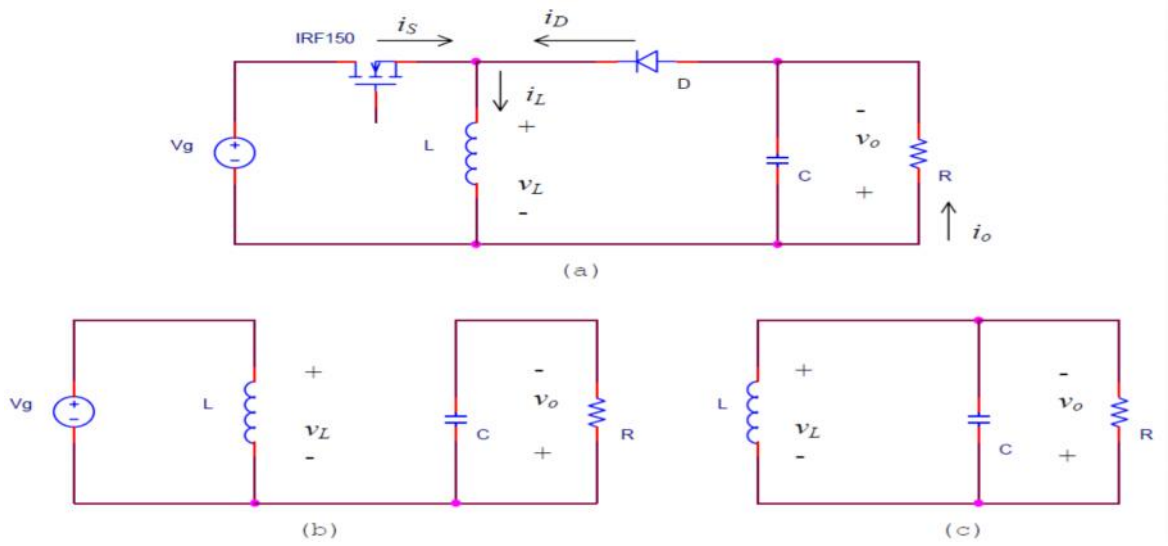

Fig-2.6-: (a) Buck-Boost converter circuit

(b) When the switch is ON (c) When the switch is OFF. [6]

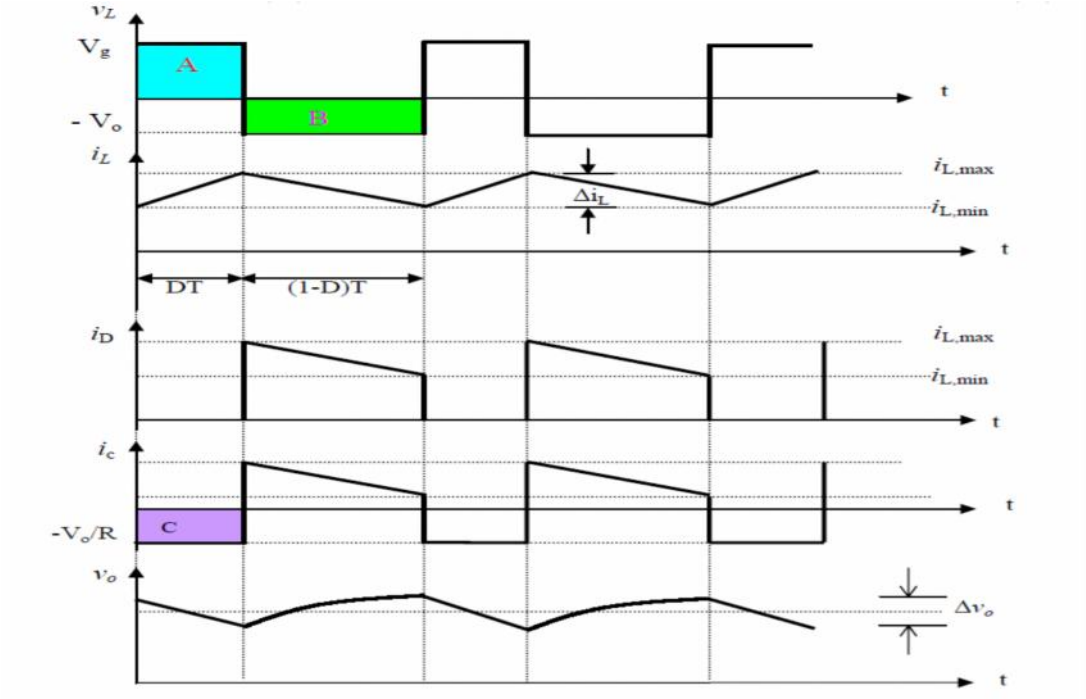

Fig-2.7-: Current and voltage waveforms in the buck-boost converter. [6]

Equating the integral of the inductor voltage over one time period to zero (Volt-second balance) yields

$$\int_0^T v_L(t)dt = \int_0^{Ton} v_L(t)dt + \int_0^{Toff} v_L(t)dt = 0 \quad (2.7)$$

$$V_L = DT \cdot V_g + (1 - D)T \cdot (-V_o) = 0 \Rightarrow V_o = \frac{D}{1-D} \cdot V_g \quad (2.8)$$

The conversion ratio can be determined to be:

$$M(D) = \frac{V_o}{V_g} = \frac{D}{1-D} \quad (2.9)$$

2.3 DC to AC converter: [8]

The DC to AC converters also called the inverter, is a circuit used to convert the DC power into AC power, we utilize it because the most of useful electrical elements are consume an AC power in its operation. The inverter may be single or multi-phase. Several topologies exist for both single phase and multi-phase inverters. An example is a full bridge single phase inverter in Fig. It consists of four switches that are turned ON and OFF. The upper and lower switches are never on at the same time to avoid short-circuiting the DC source.

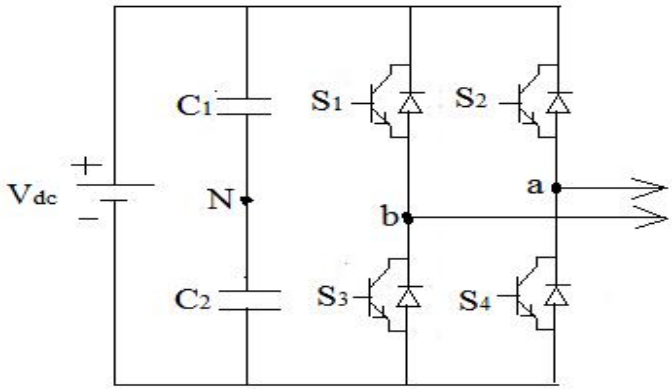

Fig-2.8-: DC to AC converter circuit. [8]

State#	Switches position			
1	S1 and S4 are on and S2 and S3 are off	Vdc/2	-Vdc/2	Vdc
2	S3 and S2 are on and S1 and S4 are off	-Vdc/2	Vdc/2	-Vdc
3	S1 and S2 are on and S3 and S4 are off	Vdc/2	Vdc/2	0
4	S3 and S4 are on and S1 and S2 are off	-Vdc/2	-Vdc/2	0
5	S1, S2, S3 and S4 are all off	-Vdc/2	Vdc/2	-Vdc
		Vdc/2	-Vdc/2	Vdc

Table.1: Inverter switches state. [8]

2.4 DC to DC converter for PV system

The heart of MPPT hardware of PV system is a switch-mode DC-DC converter. For example some converters are only suitable for stepping down the voltage (buck), while others are only suitable for stepping it up (boost), a third group can be used for either stepping up or stepping down (buck-boost). Generally in grid-connected systems where the MPPT system is part a boost converter is utilized which maintains a high voltage even if the array voltage falls. The buck converter is usually used for charging batteries and for water pumping system because lowers voltage than the voltage sources are required.

2.4.1 Simulation of a photovoltaic solar system:

Selection of components: The value L of the inductor required to ensure the converter operating in the continuous conduction mode is calculated such that the peak inductor current at maximum input power does not exceed the power switch current rating. Hence, L is calculated as: [16]

$$L_{boundary} = \frac{V_{om}(1-D_m)D_m}{2f|\Delta I_{Lm}|} \quad (2.10)$$

Where f, D_m,ΔI_{Lm} , $V_{om}$and I_{om} are respectively, switching frequency, duty cycle at maximum converter input power, peak-to-peak ripple of the inductor current, maximum of dc component of the output voltage, and dc component of the output current at maximum output power.

Taking into account that the ripple of the PV output current must be less than 2% of its mean value [16], the input capacitor value is given by:

$$C_{inmin} = \frac{I_{om}D_m^2}{0.02(1-D_n)V_{inm}2f} \quad (2.11)$$

For any inductance larger than this value the boost converter will operate in the continuous conduction mode. A much larger filter capacitance C is required as the current supplied to the output RC circuit is discontinuous.

The limiting value is given by [16]:

$$C_{outmin} = \frac{DV_{out}}{V_r Rf} \quad (2.12)$$

2.5 The simulated circuit and result using Matlab/Simulink:

The Figure-2.9- shows the circuit that has been simulated at the nominal condition (T=25°and G=1000W/m^2), and Fig.2.10 shows the simulation result for the input and output voltage, current and the power.

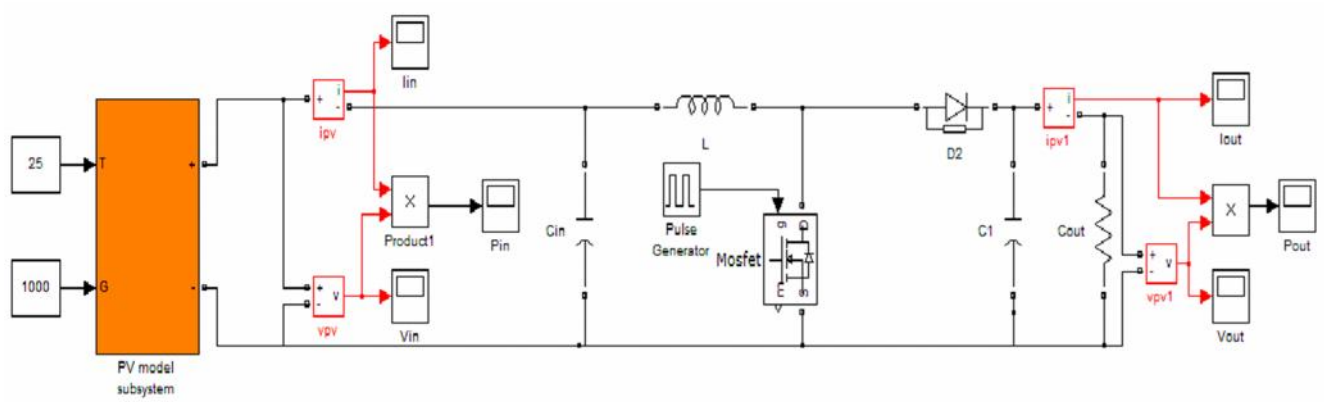

Fig-2.9-: PV system Simulink model (Without MPPT).

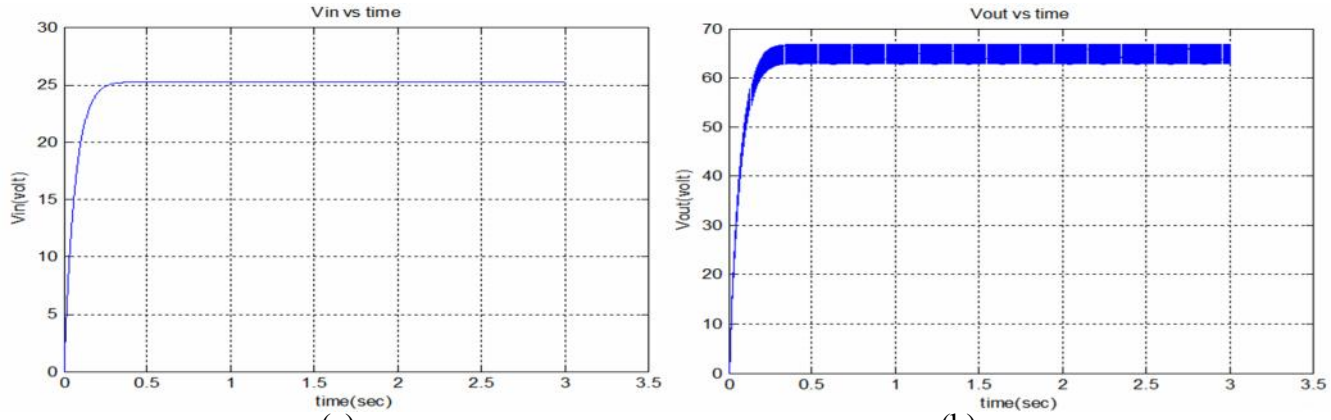

(a) (b)

Fig-2.10- : PV system input voltage (a), and output voltage (b).

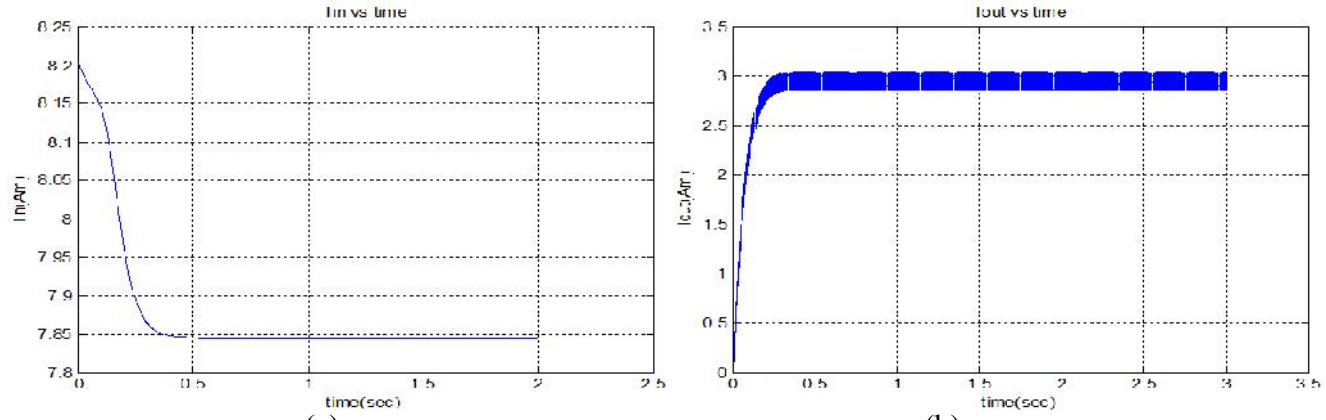

(a) (b)

Fig-2.11- : PV system input current (a), and output current (b) .

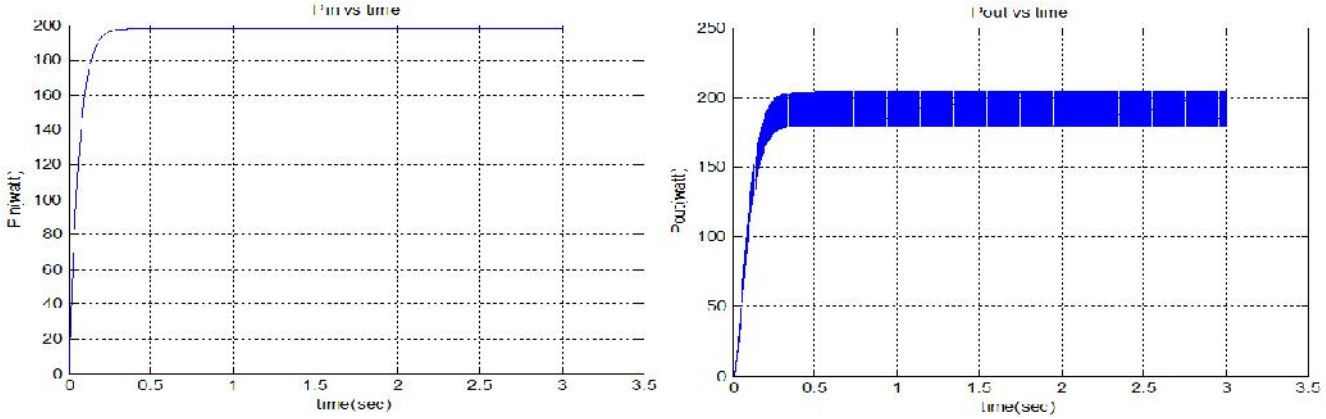

(a) (b)

Fig-2.12- : PV system input power (a), and output power (b).

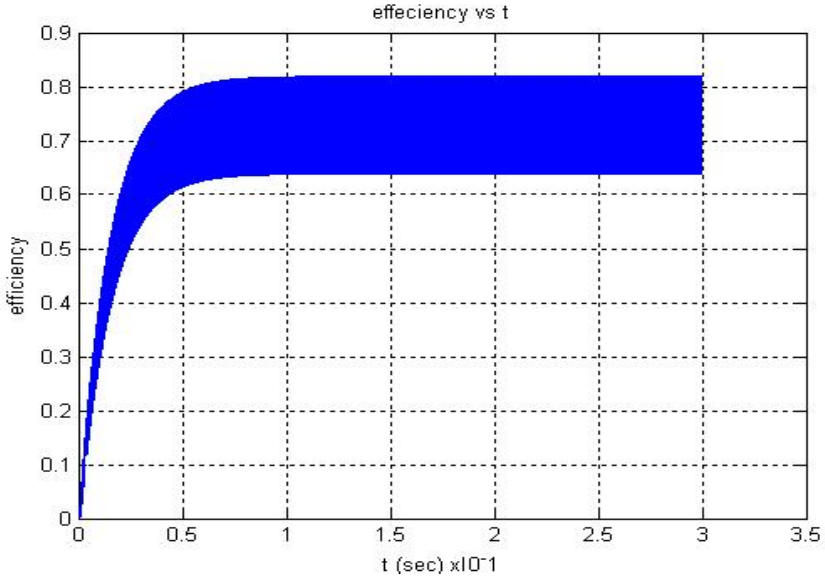

Fig-2.13-: the efficiency of the PV system without MPPT.

2.6 Conclusion

The simulation of the PV system gives good results in nominal conditions with their equivalent duty cycle. But, the efficiency shown in the simulation is much stressed and has high ripples which are around 20% in addition to its value which is 70% be used the boost chopper consumes high power as losses that's why we should introduce a technique to reduce them and increase the efficiency. The MPPT technique will ensure maximum power at all times and increase the efficiency of the boost chopper.

3.1 Maximum Power Point Tracking algorithms

3.1.1 Introduction:

As it was previously mentioned, MPPT algorithms are necessary in PV applications because the MPP of solar panel varies with irradiance and temperature. So the use of MPPT algorithm is required in order to obtain maximum power from the solar array.

Over the last decades many techniques to find the MPP have been developed and published. These techniques differ in many aspects such as the complexity, cost, and convergence speed, correct tracking when irradiation and/or temperature changes, hardware needed for the implementation or popularity.

In this chapter, we will present some of the most widely known and used MPPT techniques.

3.1.2 Fractional open-circuit voltage:

This method uses an approximate linear relationship between the MPP voltage (V_{MPP}) and the open circuit voltage (V_{OC}), which is function of the irradiance and the temperature [10]:

$$V_{MPP} \approx K_1 V_{OC} \quad (3.1)$$

Where K_1 is a constant depending on the characteristics of the PV panel and it has to be determined by conducting several experiments and determine the V_{MPP} and V_{OC} for different levels of irradiation and different temperatures. The constant K_1 has been reported to be between [0.71; 0.78]. [10]

Once the value of the constant K_1 is known, the MPP voltage (V_{MPP}) can be determined periodically by measuring V_{OC}. In doing so the power converter has to be shutdown momentarily which causes a loss of power. In addition, this method is not capable of reaching the real MPP point because the relationship is only an approximation.

Depending on the application, this technique can be used because it's very easy to implement and it is cheap (it does not require DSP or microcontroller control and just one voltage sensor is used), however, this method is not valid under partial shading because the value of K_1 changes.

The fig-3.1.2- shows the scheme of the Fractional open-circuit voltage method:

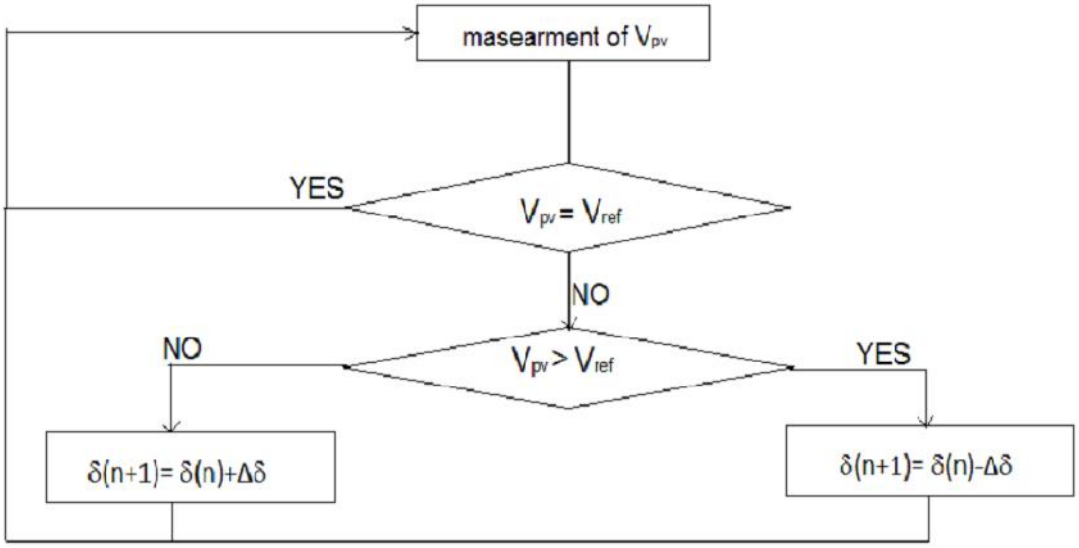

Fig-3.1.2-: Flowchart of the Fractional open-circuit voltage algorithm.[11]

3.1.3 Fractional short-circuit current:

In the same manner of fractional open-circuit voltage, there's a relationship, under varying atmospheric conditions, between the short circuit current I_{SC} and the MPP current, I_{MPP} as shown by:

$$I_{MPP} = K_2 * I_{SC}. \quad (3.2)$$

Where, the constant K2 has been reported to be between [0.78; 0.92] [10].

Measuring the short circuit I_{SC} current while the system is operating presents a problem. It is usually requires adding an additional switch to the power converter to periodically short the PV array and measure I_{SC}. One other handicap is that the real MPP is not reached because the proportional relationship is an approximation. Fig-3.1.3- shows the scheme of the Fractional short-circuit current algorithm.

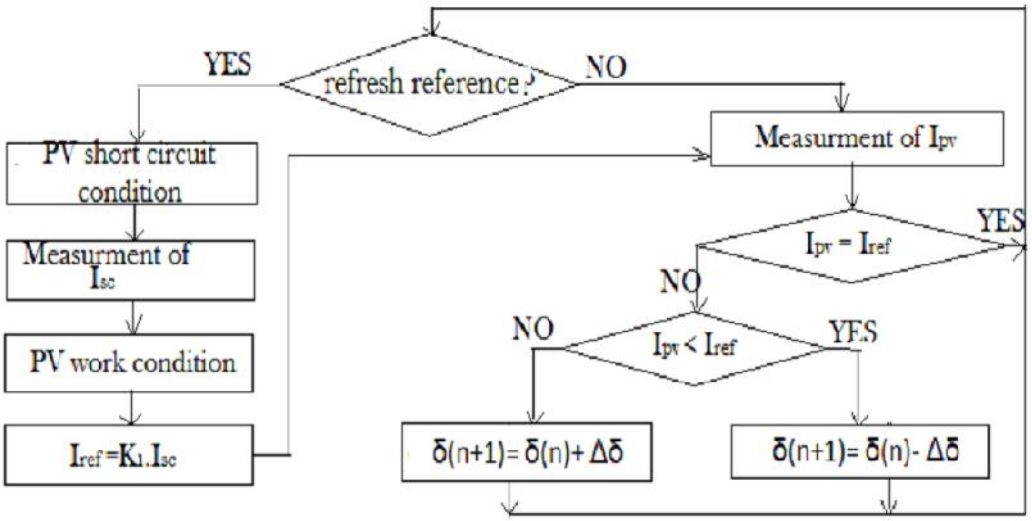

Fig-3.1.3-: Flowchart of the Fractional short-circuit current algorithm[11]

3.1.4 Hill-climbing techniques:[9]

The Perturb and observe (P&O) technique and incremental conductance (InCond) are both based on Hill-climbing principal, which consists of moving the operating point in the direction in which the power increases. Hill-climbing techniques are the most popular MPPT methods due their ease of implementation and the good performance when the irradiance is constant. The advantages of both methods are the simplicity and the low computational power needed.

3.1.4.1 Perturb and observe (P&O):

The P&O technique involves a perturbation in the duty cycle of the power converter (DC/DC converter), the sign of the last perturbation and the sign of the last increment in the power decide what the next perturbation should be. Such that if there is an increment in the power, the perturbation should be kept in the same direction and if the power decreases, then the next perturbation should be in the opposite direction.

Based on these facts, the algorithm is implemented; the process is repeated until the MPP is reached. Then the operating point oscillates around the MPP and this problem is also common to the InCond method, a scheme of the algorithm is shown in the fig –3.1.4.1-:

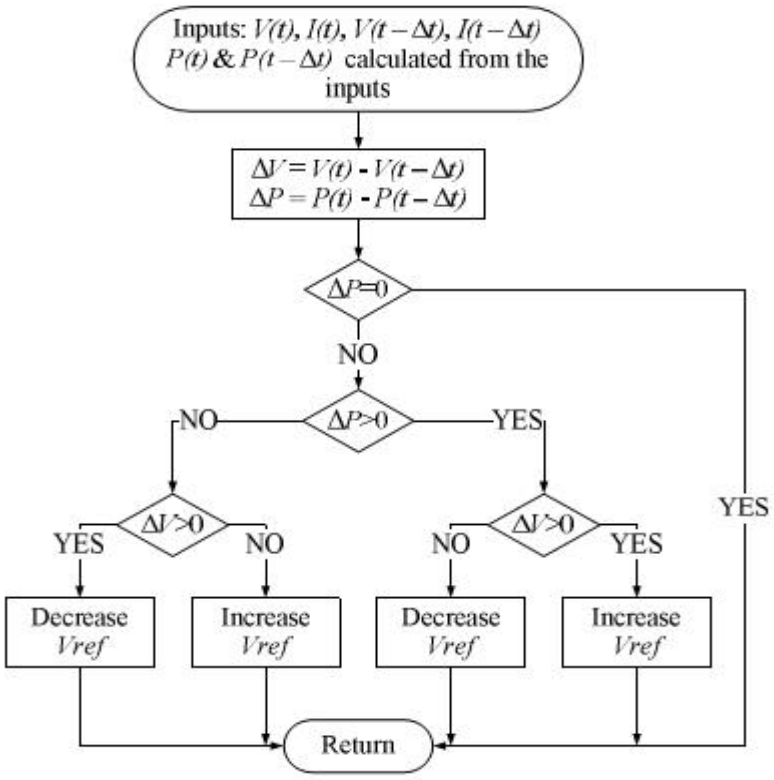

Fig-3.1.4.1-: Flowchart of the P&O algorithm. [9]

3.4.1.2 Incremental conductance method: [9]

The Incremental conductance (InCond) method is based on the fact that the sum of the instantaneous conductance I/V and the incremental conductance ΔI/ΔV is zero at the MPP, negative on the right side of the MPP, and positive on the left side of the MPP. This can be summarized as follows:

$$\begin{cases} I/V + \Delta I/\Delta V < 0, \text{ right of MPP.} \\ I/V + \Delta I/\Delta V = 0, \text{ at MPP.} \\ I/V + \Delta I/\Delta V > 0, \text{ left of MPP.} \end{cases} \quad (3.3)$$

From these characteristics, it's seen that |dP/dV| decreases as MPP is approached and increases when the operating point moves away from MPP. This relation can be given by:

$$\begin{cases} dP/dV<0, \text{ right of MPP.} \\ dP/dV=0, \text{ at MPP.} \\ dP/dV>0, \text{ left of MPP.} \end{cases} \qquad (3.4)$$

In order to obtain the operating MPP, dP/dV should be calculated:

$$\frac{dP}{dV} = \frac{d(V\,I)}{d\,V} = I + V\frac{dI}{dV} \qquad (3.5)$$

This method suffers from the same drawbacks of the P&O method, especially that it can easily lose to track the MPP when there's a rapidly change in the irradiance, so the changes in the voltage and current are not only due to the perturbation of the voltage. As a consequence it is not possible for the algorithms to determine whether the change in the power is due to its own voltage increment or due to the change in the irradiation.

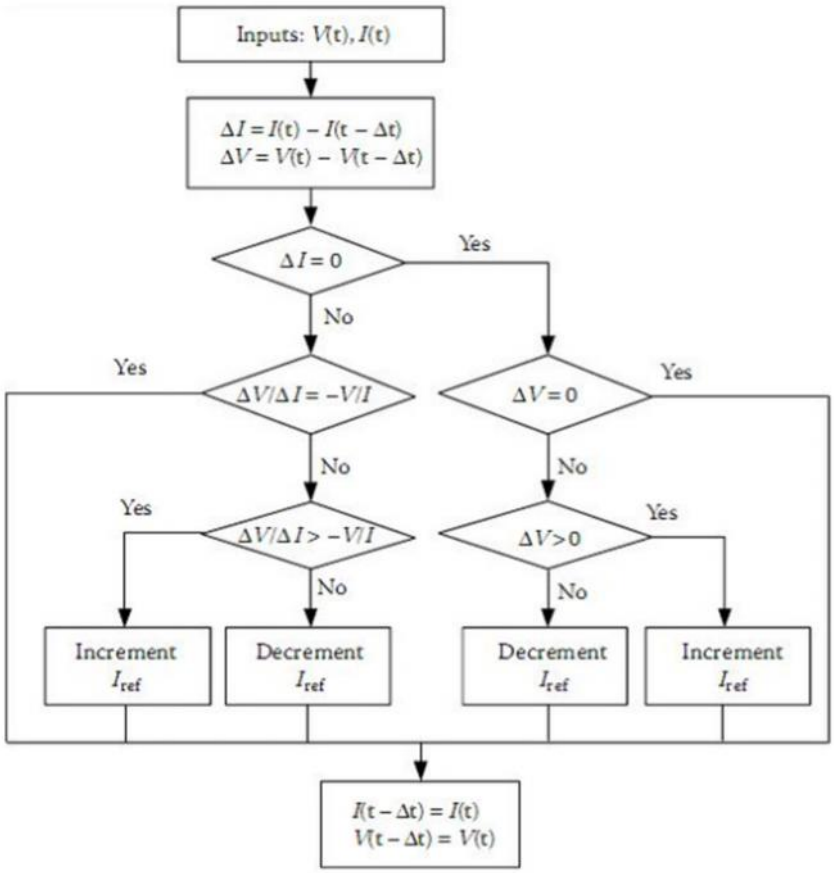

Fig-3.1.4.2-: Flowchart of the incremental inductance method algorithm. [4]

3.2 Sun Tracking System

3.2.1 Introduction:

The electric power generated by a photovoltaic panel strongly depends on the sunlight and to a lesser degree of cell temperature; these two variables influencing the behaviour of the system and show daily and seasonal fluctuations. For these reasons, the photovoltaic panel can provide maximum power for special voltage and a definite current; this operation at maximum power depends on the load at its terminals. For this purpose and according to the type of the load, a control device should be integrated into the converter control circuit. The latter must be able to operate the photovoltaic panel at its maximum power. The method of monitoring or "Tracking" known as **MPPT** (Maximum Power Point Tracking) is based on the use of a search algorithm of maximum power curve of the photovoltaic panel.In order to collect the maximum energy, we also use devices called solar tracking systems 'sun tracking systems.The solar tracking system should be adjusted so that the **PV** source is always aimed precisely towards the sun.

3.2.2 Importance of solar tracking:

The sun moves during the day and the seasons. The solar panel, however, is usually located in a fixed position, resulting in valuable energy losses.A fixed installation, oriented, in the ideal case, to the south delivers a power that grows very slowly early and strongly decreases the afternoon.

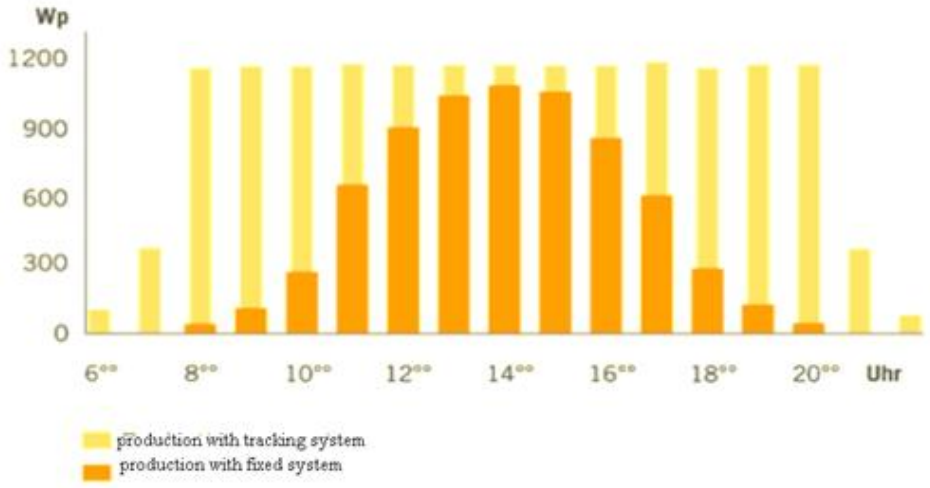

Figure 3.2.2 : comparison chart between single-tracking system and fixed system production.

The role of the tracking mechanism is to adjust the position of the sensor so that incident solar radiation is always perpendicular to the reflector to capture the maximum of the incident ray.

3.2.3- Directions of solar panels:

3.2.3.1- Selection orientation modules:

The orientation of the modules must be facing south for sites in the northern hemisphere and due north to the southern hemisphere sites using a compass is highly recommended to avoid any approximation that might introduce loss Consecutive power misdirecting.

3.2.3.2- Selection module tilt : [5]

For the modules produce maximum energy requires that the surface is perpendicular to the sun. We must therefore tilt the modules so that they are facing the sun. The value of inclination corresponds to the angle between the modules with the horizontal. Since it is difficult to change several times in the coures of the year the inclination of the modules are generally selected a mean value for the whole year.

3.2.3.3 -Apparent trajectory of sun:

For an observer located on the surface of the earth, the sun describes an apparent trajectory that depends on latitude (height) and longitude (azimuth) of where it is located. Recall that the latitude is the angular distance from any point of the globe over the equator **(0** to **90** in the northern hemisphere) .when a longitude is also an angle, gives to the meridian Greenwich in moves eastward The apparent movement of the sun and about **240** in azimuth and **70** in elevation latitudes. The sun moves during the day and following the season **Figure 4-2** .the solar panel, however, is usually located in a fixed position, resulting in valuable energy losses. A fixed installation, oriented, in the ideal case, to the south delivers power that believes very slowly early morning strongly afternoon. An important part of the recoverable energy is lost.

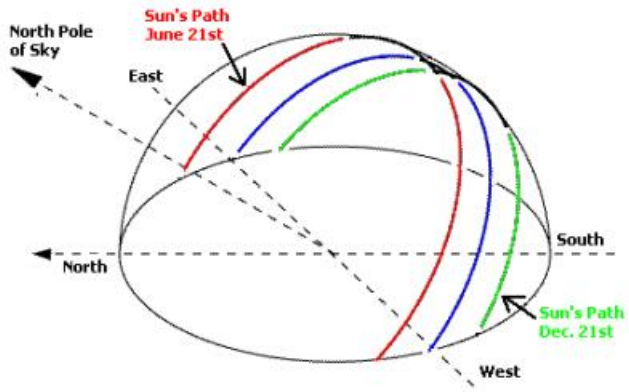

Figure 3.2.3.: defining the position of the sun

If the installation is constantly orient toward the sun; it generates maximum power. A fixed installation **1KW** is oriented optimal way, produced a day of sunshine, about **5KW** solar power.The same installation with **1KW** follower however provides up to **10KW** per day.That is to say **50%** of energy gain more. Thus, only automatic rotation may allow the solar panel delivered maximum power.

3.2.4- Type of orientation [6]:

The solar panel to follow the sun, it is necessary that it receives rays are perpendicular to it. For this, we must make the mobile panel, we must design a mechanism that would allow the panel to follow the sun's position in the following

day (east to west) and its height in the sky that changes with the solar declination (angle varying due to the inclination of the earth).

3.2.4.1- Single axis orientation [7]:

A motor provides the rotation of a shaft on which is fixed the panel. This will allow the panel to go from east to west.

Figure 3.2.4.1 : Orientation with1 axis

3.2.4.2- Dual axis orientation [8] :

For rotation two axes must be used two motor. The first ensures the rotation East / West and second North / South position

Figure 3.2.4.2 : dual axis Orientation

3.2.5 - The photoresistor (LDR) :

In order to assure the position of the sun, the drive mechanism with the information of the position of the latter, which must use light-sensitive sensors that ensuring the adjustment of the mechanism to ensure an angle of incidence equals. A photoresistor is a component whose value in ohms depends on the light to which it is exposed. It also refers to the **LDR** (Light Dependent Resistor). The main use of the photocell is measuring the light intensity (camera, detection systems, metering and alarm ...). It is strongly challenged by the photodiode whose response time is much shorter. The materials used are generally sulfide or cadmium selenide which behave as semiconductors.More intense will be the luminous flux, the greater the number of electrons available to ensure the conduction will be great and the resistance of the **LDR** is inversely proportional to the received light.

3.2 Conclusion:

In this chapter, most of the developed MPPT techniques were reviewed, some of them are very similar and use the same principle but expressed in different ways, like the Hill-climbing techniques.

The most popular MPPT techniques are the P&O and the InCond, and they were selected because they are the simplest algorithms capable of finding the real MPP. Which is not the case in the fractional short-circuits current and fractional open-circuit voltage techniques, where the MPP is just an approximation and thus the tracked MPP is not the real one.

Many modifications were proposed to optimize the P&O and InCond techniques and to overcome the disadvantages of their original version, especially their limitation in tracking the real MPP under rapidly changing irradiance conditions.

4.1Introduction

In this chapter, the design and implementation of a basic electronic circuitis presented to optimize the power of a PV source of a particular system inthree actions:

- Tracking the sun through a mechanical mechanism, which permits to fix the direction of the module.
- Ensure the operation of the PV source at maximum power operating point (MPPT) using a DC / DC power converter (Buck-Boost converter).
- Display the results **Ipv**,**Vpv** and **P** to 16x2 **LCD**

Thus, the general block diagram is illustrated in the following figure:

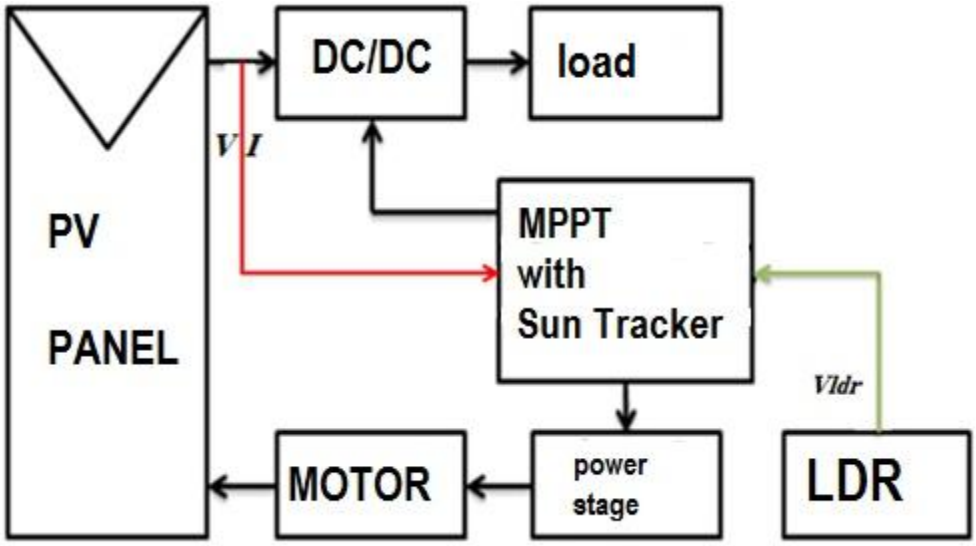

Figure 4.1: Block diagram of a PV source aided with a solar tracker and a MPPT converter.

4.2Methodology:

For the design, three main tasks were performed:

- Tracking the sun.
- Those of the MPPT function.
- Display the results using 16x2 LCD display.

- The control program ofthe microcontroller is written in C language using an editor (MikroC), which permits to have a hex code to be loaded into the PIC16F877A's EPROM.

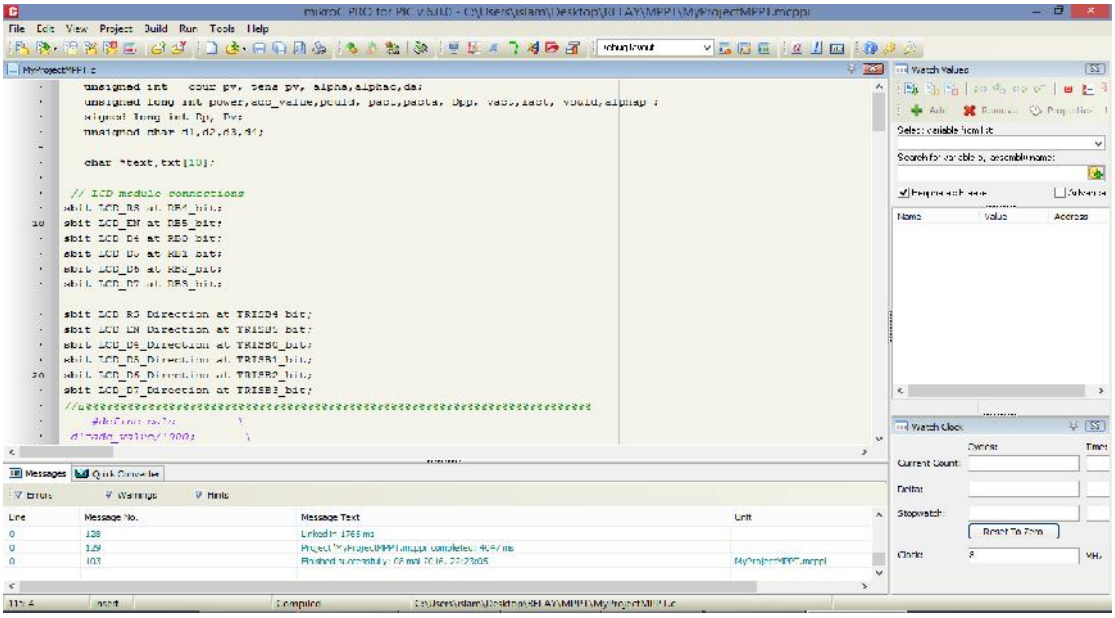

Figure 4.2.1 MikroC window

- The circuit construction is implemented using Proteus :

Proteus is software for microprocessor and microcontroller simulation, schematiccapture, and printed circuit board (PCB) design. It is developed by Labcenter Electronics. **Figure 4.2.2** shows Proteus window.

Proteus consists of a single application with many modules such asISIS Schematic Capture, PROSPICE Mixed mode SPICE simulation, ARES PCBLayout and VSM (Virtual System Modeling). This project will use ISIS SchematicCapture to design the buck converter circuit and VSM mode to simulate the project.

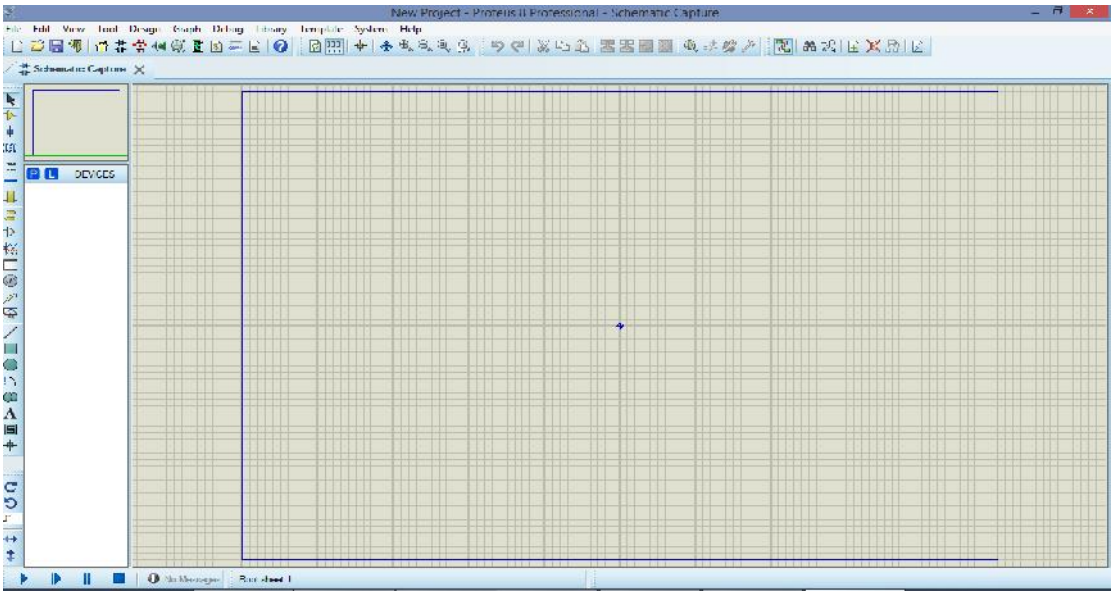

Figure 4.4.2 Proteus window

4.3 Tracking procedure:

This operation ensures tracking the sun position in a continuous or discrete motion such that the PV source still faces the sun. The automatic control of the sun tracking system comprises the following parts:

- Sensors and matchinglevel.
- Power stage.
- Electro mechanicalmechanism.

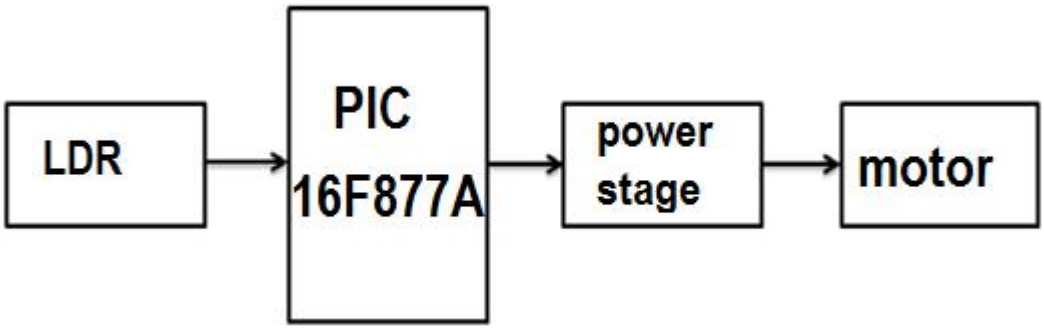

Figure 4.3.1- Schematic Diagram of the sun tracker.

The LDR circuit serves as an interface between the solar collector and the microcontroller. The sensor information, after conditioning, is transmitted to the microcontroller, which operates with the transition of the voltage level (0V, 5V).

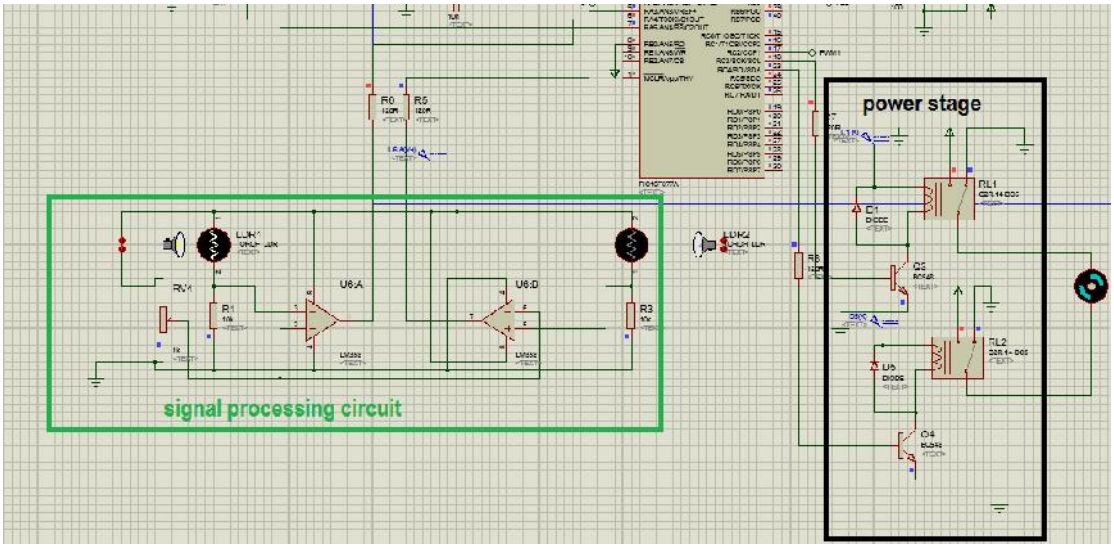

Figure 4.3.2- The circuit of the tracking system

4.3.1 Signal processing circuit:

According to the solar collector position (**Figure 4.3.2**) shows the two comparators (without feedback loop) compare the voltage at their inputInput variable without reversing the effect of the illumination (varies the ratio of the voltage divider 'LDR1, R1, LDR2, R3' ')

- The input of the inverters whose input voltage is determined by RV1 that the voltage threshold is halfway between the position A / B and the optimal.

Table 3-1 below summarizes the state of the output PDO according to sensor position and the direction of motor rotation.

Position	OPAMP1	OPAMP2	Relay 1	Relay 2	Engine
A	1	0	1	0	Works
B	0	1	0	1	Works
C	0	0	0	0	Stops

Table 3-1: Output state of OPAMP PDO depending on the position of capture

4.3.2 The power stage:

The power stage is composed of circuit, which ensures the driving force for the motor to seek the desired direction.

According to the variation of sun, there are TR1or TR2 that track all actions to therelay which bias the motor drive through the contacts RL1 or RL2. The base resistors R2 and R4 must be determined such that the switches transistor TR1 and TR2 are in saturation mode.

4.3.3 the sun tracker Algorithm:

The sun tracking algorithm is shown in the figure III-8, and is translated to a program that ensures the position of the mechanism.

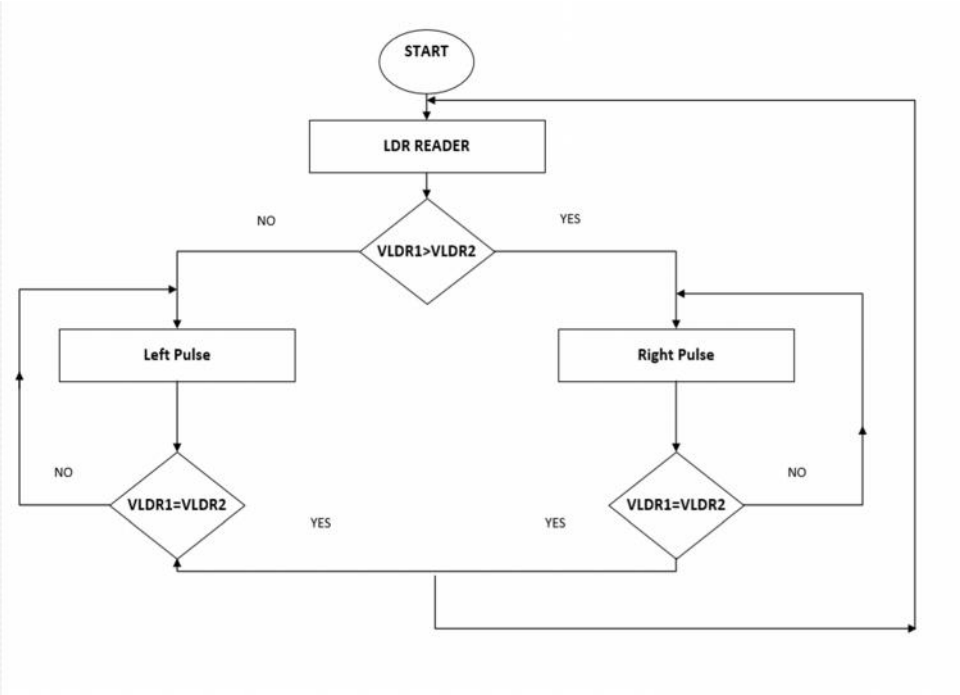

Figure 4.3.3: Algorithm of the sun tracker.

4.4 Digital MPPT procedure:

The approach to achieve the MPPT as explained in Chapter 3 Section 3.1.4.1 (Perturbation and Observation algorithm),The buck–boost converter is a two fuctions converter type that has an output voltage magnitude that is either greater than or less than the input voltage magnitude. It is a switched mode power supply with a similar circuit topology to the boost converter and the buck converter. The output voltage is adjustable based on the duty cycle of the switching transistor.

4.4.1-The power stage:

The diagram of the buck converter is included below:

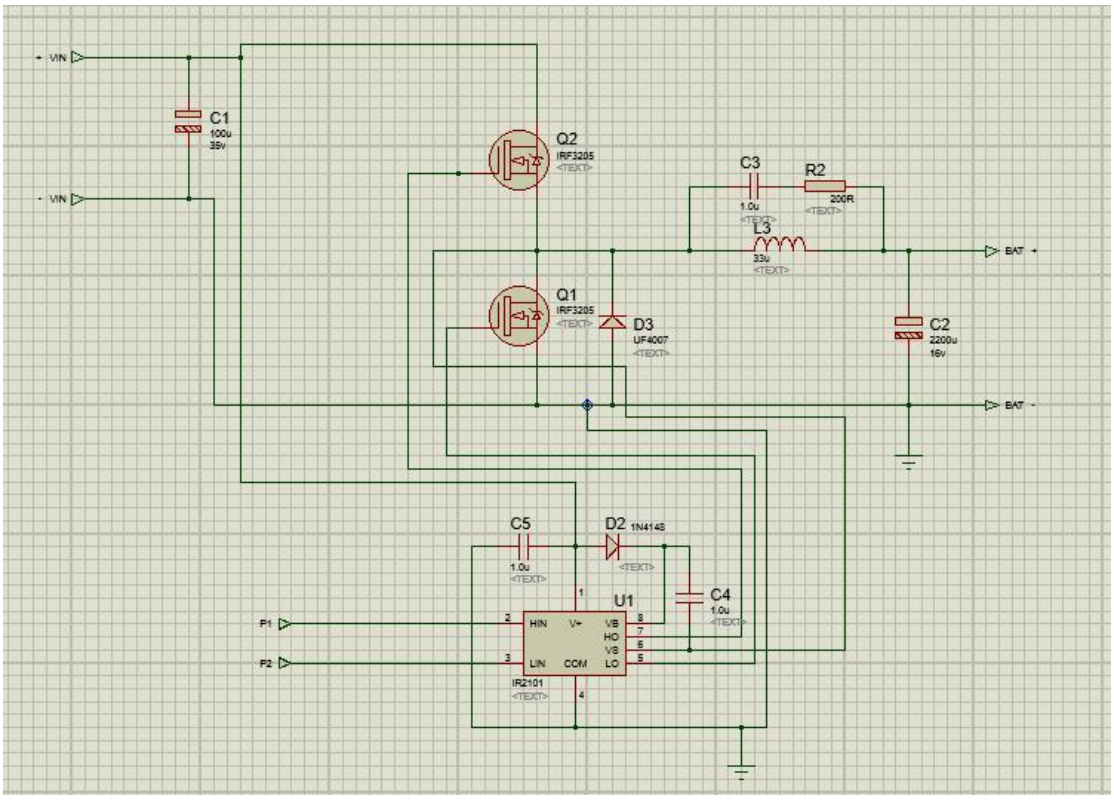

Figure 4.4.1 schematic of Buck-Boost converter

➢ The Choice of the MOSFET

We chose the IRF3205 MOSFET switch as static. Its main features are:

- Ultra low on resistance .
- 175°C operating temperature .
- Fast switching.

The MOSFET is driven by MOSFET driver

➢ The MOSFET's driver selection

Driver MOSFETs that we have selected is the IR2101, This driver was chosen because it is dedicated to control a Buck-Boost converter, The IR2101 are high voltage, high speed power MOSFET and IGBT driver with independent high and low side referenced output channels. The logic input is compatible with standard CMOS or LSTTL output, down to 3.3V logic. The output drivers feature a high pulse current buffer stage designed for minimum driver cross-conduction.

The floating channel can be user to drive an N-channel power MOSFET or IGBT in the high side configuration, which operates up to 600 Volts.

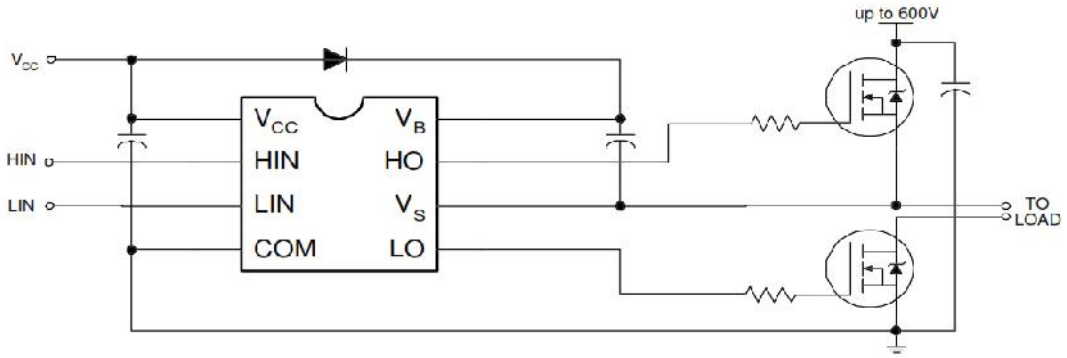

Figure 4.4.2 IR2101 MOSFET's driver

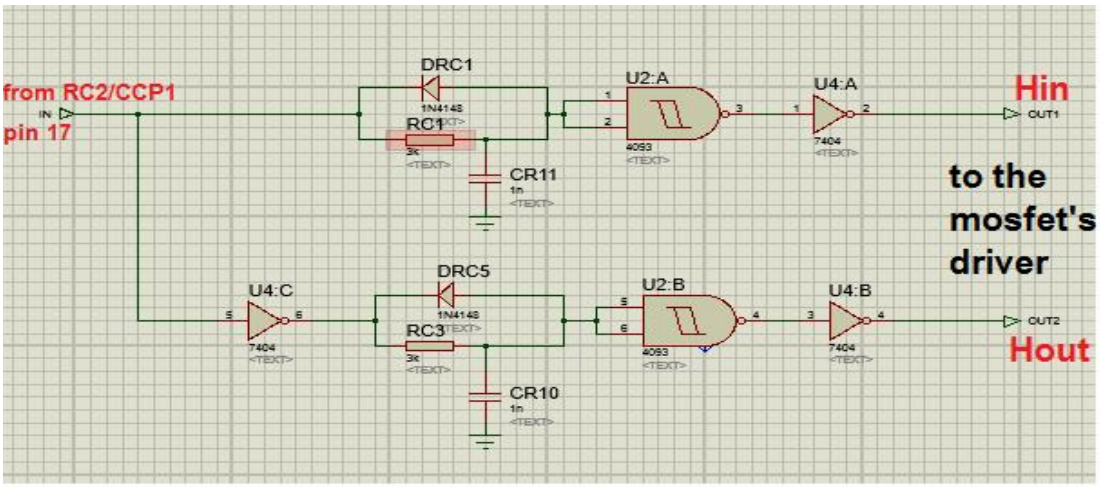

Figure 4.4.3 the PWM circuit

4.4.2 – The PV module:

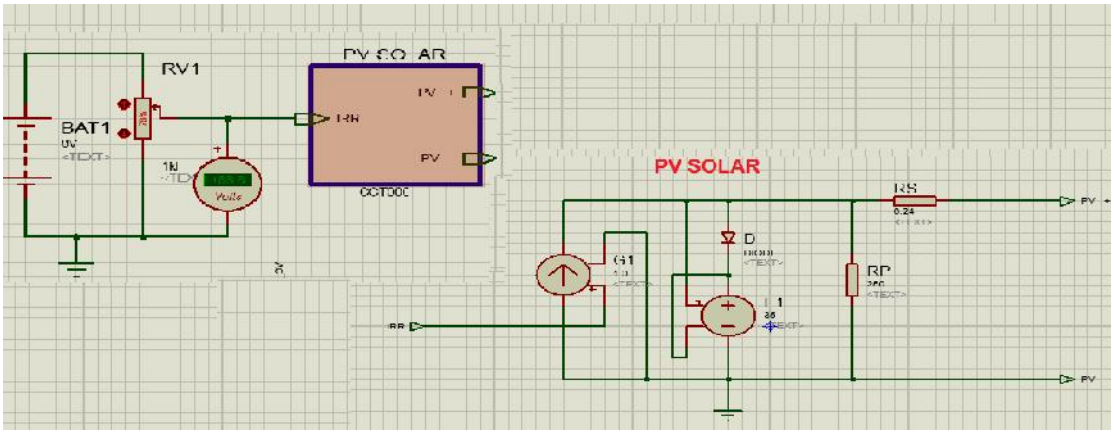

Figure 4.4.2 The PV module circuit

4.4.3- The control stage:

The control unit consists of two essential parts: the measure circuit that reads the voltage and current of the PV panel. The second part, which is in fact this block is formed by a PIC 16F877A, to program the MPPT algorithms.

4.4.3.1- The measure circuit:

- **voltage Measurements**

The voltage measurement is needed to calculate the power produced by the PV source. PIC microcontrollers Mid-Range family are able to measure a voltage because they are aided by Analog to Digital converter. However, the voltage to be measured for this application exceeds the tolerance level of the PIC , which is 5V. A voltage higher than 5V may destroy the PIC.

To avoid this, we should use a voltage divider that will decrease the voltage to be measured to the tolerance level of the PIC.

We have seen that for the measurement of voltages, one must use a voltage divider to keep safety for the PIC.

For a safe operation, we choose 5V PIC side as the maximum value. To obtain the value of the necessary resistance, we use the equation:

$$\frac{U_{PIC}}{U_{PV}} = \frac{R_2}{R_1+R_2} \quad \textbf{(4.4)}$$

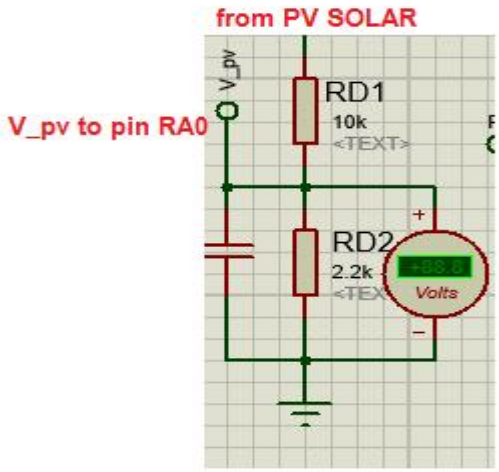

Figure 4.4.3.1 voltage overflow schematic

➢ **Current Measurements :**

PIC microcontrollers are not able to measure a current. An indirect method must be used to accomplish this task.

We choose to use a current sensor MAX4173T, its main features:

- Low-cost
- Compact Current-Sense solution .
- Wide 0 to +28V Common-Mode Range.

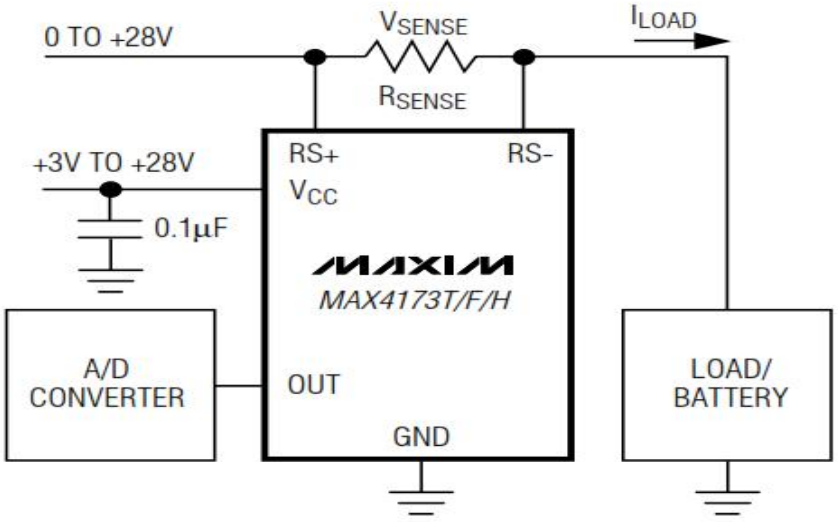

Figure 4.4.3.2 MAX4173 current sensor

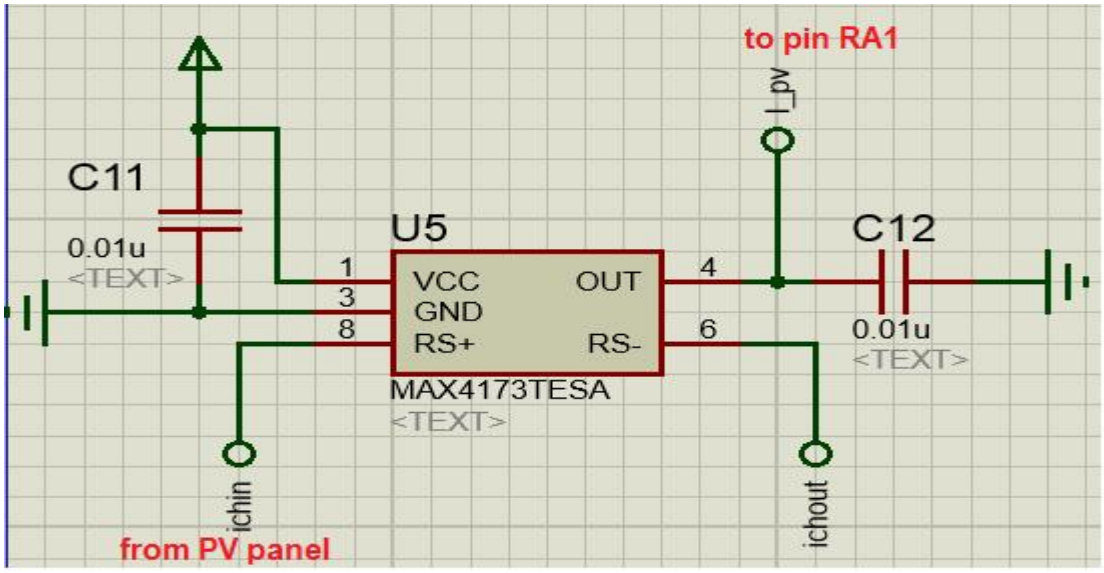

Figure 4.4.3.3 Current sensor connection

4.5-Microcontroller:

The PIC microcontrollers are RISC (Reduce Instructions Construction Set), or game's component reduced instruction. The advantage is that the more one reduces the number of instructions in addition to their decoding is faster, which increases the speed of operation.

The PIC family is divided into 3 main categories:

- The family Base Line: using words of 12-bit instructions.
- Mid-Range Family: which uses 14-bit words.
- High-End Family: which uses 16-bit words.

  The PIC are STATIC components, they can operate with clock frequencies from DC to a specific frequency to each circuit max.

4.5.1-PIC Choices:

According to the tender specifications and the integrated function we can choose such a peak as techno economic development compelled games at our disposal we have several circuit. As PIC 16F84, 16F877A, 18F225 and 18F445 doubt different functions.

For our circuit, the main functions necessary for the operation of the installation are:

- requires digital input / output
- Requires the presence of an A / D converter (to reduce the I and V).
- Games interruption.
- The presence of a PWM generator is preferable.

According to the available component, we chose the 16F877A peak that meets these conditions while remaining affordable price point of view.

4.5.2- PIC16f877 Features:

- Power consumption: less than 2mA 5V to 4 MHz
- Architecture RISC: 35 Term 1 or 2 instruction cycles.
- Cycle time: Time of the quartz oscillator divided by 4 or 200 ns for a quartz 20MHz.
- Two separate buses for program code and data.

- Instruction code: 14-bit word and the program counter (PC) of 13 bits, which allows addressing 8K words (H'0000 'to h'1FFF') - Bus DATA 8 bits.
- 33 Arrival-Departure bidirectional ports, which can produce 25 mA per output. PORTA = 6bits and PORTB PORTC and PORTD PORTE = 8 bits = 3 bits for the 16F877 and 22 I / O only for the 16F876.
- 4 interrupt sources:
- External pin through shared with Port B PB0
- For bit status change of the Port B: PB5 PB4PB6 or PB7
- By an integrated device in the chip: Data EEPROM write complete, analog conversion is complete, USART or I2C reception.
- By Timer over Flow
- 28-bit counters and one 16-bit counter with pre programmable divider.
- Analog 10 bits to 8 entries for the 16F877 and 4 entries for the 16F876.
- UART for synchronous or asynchronous serial transmission.
- I2C interface.
- 2 PWM modules with a resolution of 10 bits.
- Interface with other micro: 8 bits+ 3 control bits R / W and CS.
- 368 Bytes of RAM
- 256 Bytes EEPROM Data.
- 8K words of 14 bits Flash EEPROM for the program (h'0000 'to h'1FFF').

- 1 working register W and file register F to access the RAM or internal registers of the PIC. Both are 8-bit registers.

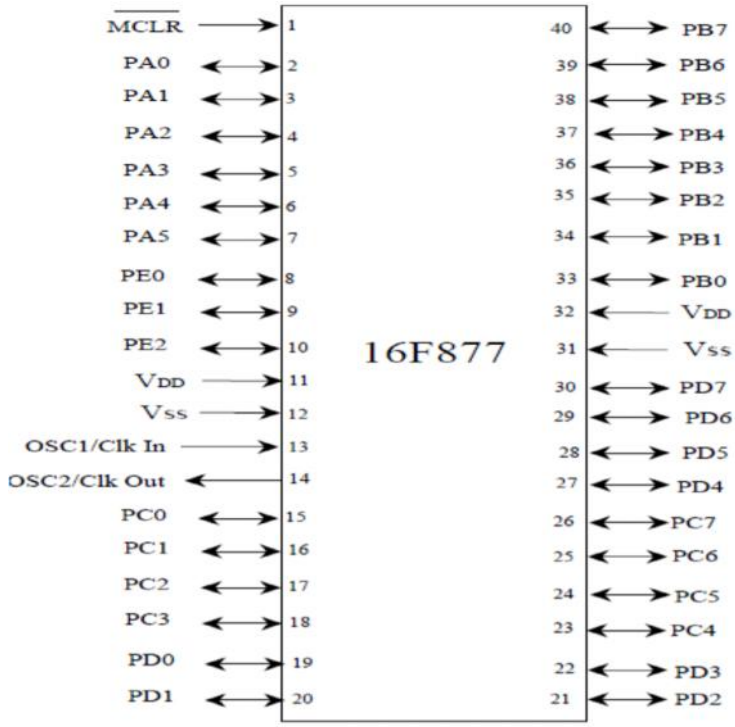

Figure 4.5.2 PIC 16F877A pins

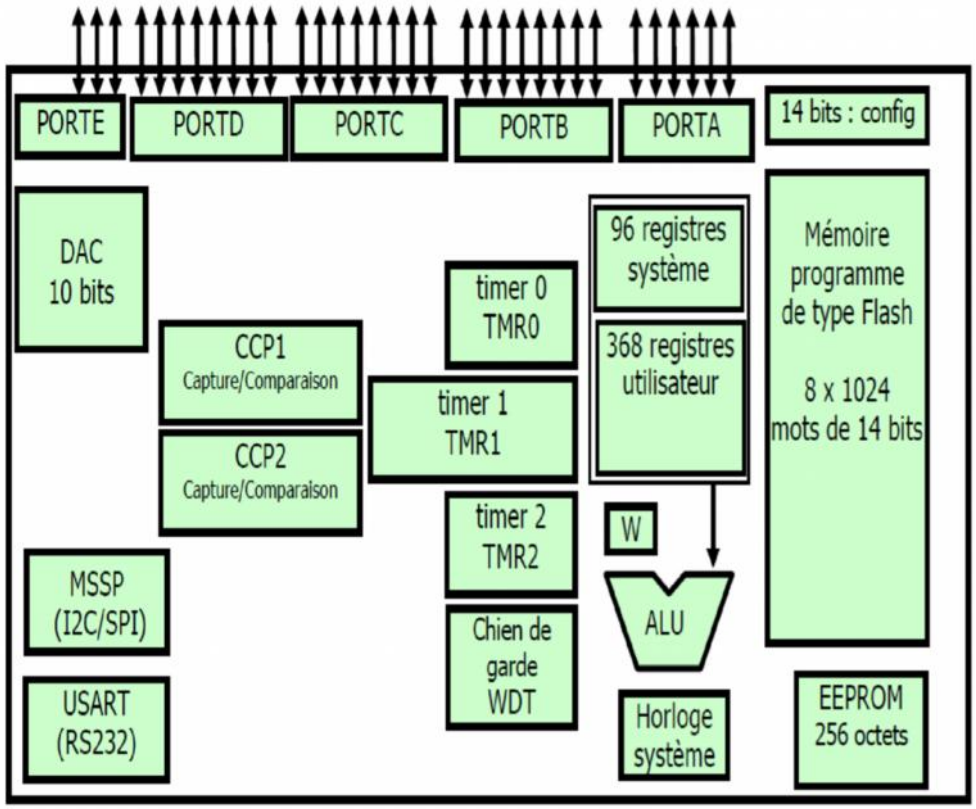

Figure 4.5.3: The components of the PIC 16F877A

4.5.3- General Description of PIC 16F877:

a) The Clock:

The clock can be either internal or external. The internal clock comprises a crystal oscillator or with an RC oscillator. With the quartz oscillator, one can have frequencies up to 20 MHz depending on the type μ. The low pass filter (R, C1, and C2) limits the harmonic due to clipping and reduces the amplitude of the oscillation, it is not mandatory.

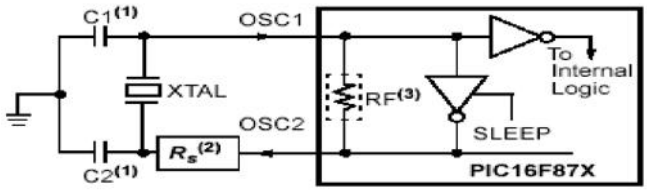

Figure 4.5.4 crystal oscillator

With an RC oscillator, Vdd, Rext and Cext determine the frequency of oscillation. It may vary slightly from one circuit to another.

In some cases, an external clock to the microcontroller can be used to synchronize the PIC on a particular process. Whatever the oscillator uses, also known as the system clock instruction clock is obtained by dividing the frequency by 4. In the rest of this document will use the term Fosc / 4 to designate the system clock.

With a 4 MHz crystal, a 1 MHz instruction clock is obtained, the time to execute a 1μs instruction.

b) The ALU and the W accumulator:

The ALU is an arithmetic and logic unit that performs 8-bit arithmetic and basic logic. The battery W is an 8-bit working register, all operations on two operands through it. One can have:

- A statement of a single operand which is typically a register located in the RAM

- A statement of 2 operands. In this case, one of the two operands is always the battery W, the other can be either a register or a constant.

For instructions whose operand is a register, the result can be recovered either in the accumulator or in the register itself.

c) Organization of the RAM:

The addressable RAM memory is 512 positions 1 byte each:

• 96 positions are reserved for the SFR (Special Function Registers) are the PIC configuration registers.

• The remaining 416 positions are the GPR registers (General Proposes Registers) or RAM user. On the 16F876 and 16F877, 3 blocks of 16 bytes each are not physically located where a user RAM capacity 368 GPR

d) EEPROM:

The PIC 16F876 / 877 has 256 bytes of data EEPROM. The first position will be the address 0, the second will address 1. . and the last will be the address 255.

e) I / O Ports:

The PIC 16F877 has 33 input pins grouped in 5 output ports PORTA, PORTB, PORTC, PORTD and PORTE. Each pin of a port can be configured as either input or output using the direction registers TRISA, TRISB, TRISC, TRISD, and TRISE.

f) Some configuration registers and bits:

STATUS	IRP	RP1	RP0	TO	PD	Z	DC	C	0001 1xxx
OPTION_REG	RBPU	INTEDG	T0CS	T0SE	PSA	PS2	PS1	PS0	1111 1111
INTCON	GIE	PEIE	T0IE	INTE	RBIE	T0IF	INTF	RBIF	0000 000x
PIE1	PSPIE	ADIE	RCIE	TXIE	SSPIE	CCP1IE	TMR2IE	TMR1IE	0000 0000
PIR1	PSPIF	ADIF	RCIF	TXIF	SSPIF	CCP1IF	TMR2IF	TMR1IF	0000 0000
PIE2	N.I.	Réservé	N.I.	EEIE	BCLIE	N.I.	N.I.	CCP2IE	-r-0 0--0
PIR2	N.I.	Réservé	N.I.	EEIF	BCLIF	N.I.	N.I.	CCP2IF	-r-0 0--0
EECON1	EEPGD	—	—	—	WRERR	WREN	WR	RD	x--- x000
TXSTA	CSRC	TX9	TXEN	SYNC	—	BRGH	TRMT	TX9D	0000 -010
RCSTA	SPEN	RX9	SREN	CREN	ADDEN	FERR	OERR	RX9D	0000 000x
CCPxCON	—	—	DCxB1	DCxB0	CCPxM3	CCPxM2	CCPxM1	CCPxM0	--00 0000
T1CON	—	—	T1CKPS1	T1CKPS0	T1OSCEN	T1SYNC	TMR1CS	TMR1ON	--00 0000
T2CON	—	TOUTPS3	TOUTPS2	TOUTPS1	TOUTPS0	TMR2ON	T2CKPS1	T2CKPS0	-000 0000
SSPCON	WCOL	SSPOV	SSPEN	CKP	SSPM3	SSPM2	SSPM1	SSPM0	0000 0000
SSPCON2	GCEN	ACKSTAT	ACKDT	ACKEN	RCEN	PEN	RSEN	SEN	0000 0000
SSPSTAT	SMP	CKE	D/A	P	S	R/W	UA	BF	0000 0000
CCP1CON	—	—	CCP1X	CCP1Y	CCP1M3	CCP1M2	CCP1M1	CCP1M0	--00 0000
TXSTA	CSRC	TX9	TXEN	SYNC	—	BRGH	TRMT	TX9D	0000 -010
RCSTA	SPEN	RX9	SREN	CREN	ADDEN	FERR	OERR	RX9D	0000 000x
CCP2CON	—	—	CCP2X	CCP2Y	CCP2M3	CCP2M2	CCP2M1	CCP2M0	--00 0000
ADCON0	ADCS1	ADCS0	CHS2	CHS1	CHS0	GO/DONE	—	ADON	0000 00-0
ADCON1	ADFM	—	—	—	PCFG3	PCFG2	PCFG1	PCFG0	0--- 0000
TRISx									1111 1111

Table 4.2: Details of SFR registers and startup states

g) Interruptions:

An interruption stops the main agenda for executing an interrupt procedure. At the end of this procedure, the microcontroller main program resumes where it left. Each interruption are associated two bits, an enable bit and flag. The first allows or not the interruption, the second allows the programmer to know which interrupt it is.

On the PIC16F876 / 877, are the interrupts are classified into two categories, primary and peripheral interruptions. The registers manage them:

INTCON	GIE	PEIE	T0IE	INTE	RBIE	T0IF	INTF	RBIF
PIE1 (bk1)	PSPIE	ADIE	RCIE	TXIE	SSPIE	CCP1IE	TMR2IE	TMR1IE
PIR1 (bk0)	PSPIF	ADIF	RCIF	TXIF	SSPIF	CCP1IF	TMR2IF	TMR1IF
PIE2 (bk0)	-	-	-	EEIE	BCLIE	-	-	CCP2IE
PIR2 (bk1)	-	-	-	EEIF	BCLIF	-	-	CCP2IF
OPTION_REG(bk1)		INTEDG						

Table 3.3: interruption of registers in the 16F877A pic

- The interruption INT (RB0 input port B)

This interruption is caused by a change of state on the RB0 input port B when it is programmed as input. In addition to its enable bit and flag INTE INTF, it is also managed by the INTEDG bit (OPTION_REG) determines the front on which the interruption occurs, 1 = amount, 0 = down.

- The RBI interruption (A RB7 RB4 of port B)

This interruption is caused by a change of state on one of the RB4 to RB7 input port B, The forehead does not matter. Associated bits are rbie (validation) and DFRP (flag)

h) CCP1 and CCP2 module (CCP: capture compare PWM)

Each of the CCP1 and CCP2 modules allows:

• Either CAPTURE in one shot the content of double register TMR1

• Either COMPARE permanently content with a 16-bit register and trigger an event when equality.

• PWM mode (pulse with modulation): This mode can generate signals in the duty cycle.

i) The conversion module A / D:

This module consists of a 10-bit Digital Analogue converter whose analog input can be connected to one of 8 (5 16F876) external analog inputs. They say we CAN has 8 channels. The analog inputs must be configured as input with the TRISA registers and / or TRISE.

4.5.3 The 16x2 LCD display:

The LCD is connected to the PIC16F877A pins as follows:

D4 to D7 are connected to RB0 to RB3.

D0 to D3 must be grounded (connected to Vss).

RS and E are connected to RB4 and RB5 respectively.

Vdd ,Vee and RW are connected to a variable resistance RV to adjust contrast

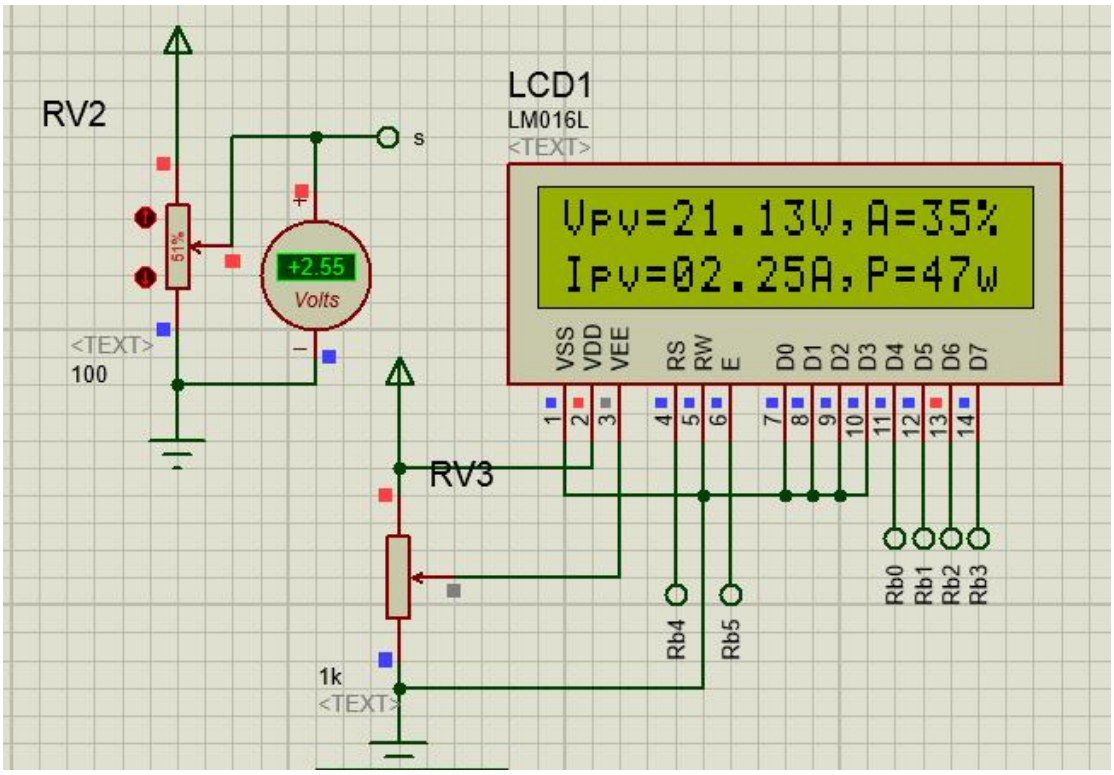

Figure 4.5.3 the 16x2 LCD interfacing with PIC16F877A.

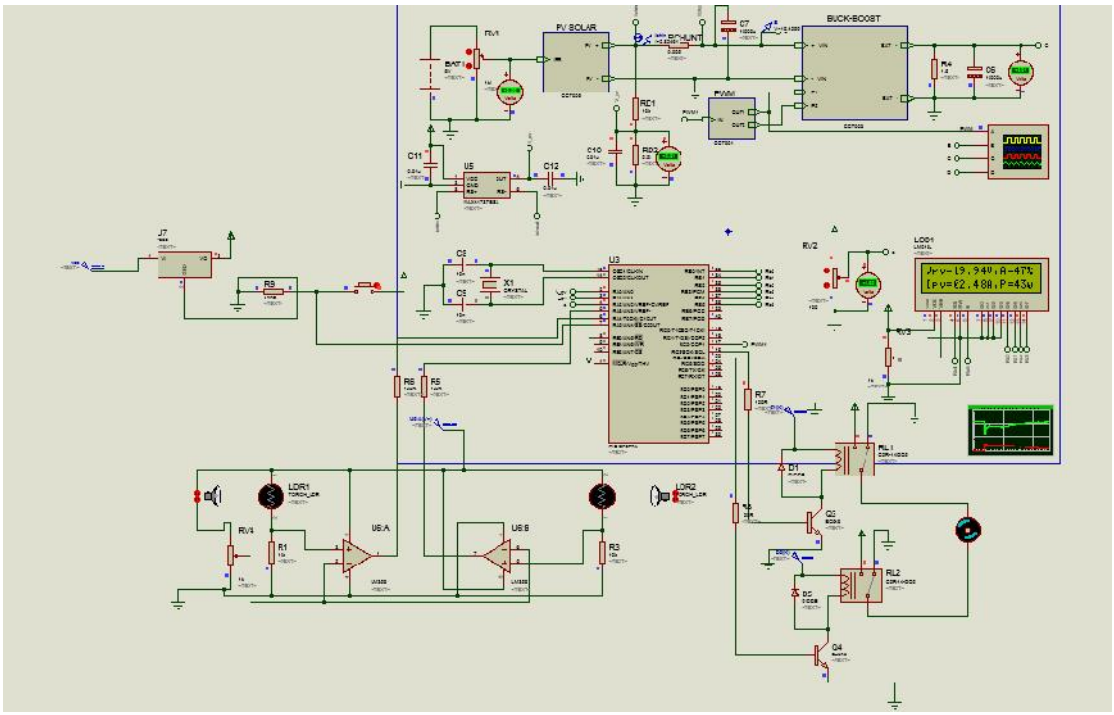

Figure 4.5.4 General schematic block diagram of sun tracker with MPPT.

4.6 Conclusion:

In this chapter we conclude that it is possible to integrate both the sun tracking and the MPPT to be performed using the same microcontroller. A mikroC codes is generated for both functions, then it is loaded in the micro controller .The model is simulated using Proteus environments for its capabilities and flexibility of manipulation. A 16xLCD display is provided to visualize simulation results to facilitate survey and efficiency of the system.

General conclusion:

The objectives of this project are achieved and demonstrate the possibility of maximizing the power produced by a PV-system using a sun tracking and MPPT at the same time. The methodology summarized in generating mikro C codes for sun tracking and MPPT algorithm .Both codes are loaded in a PIC16F877A, after a careful circuitry design of BUCK-BOOST converter including the power stage and PWM control signal generation to seek for the maximum power. A simulation model is developed using the Proteus software package .According to the outputted voltage, current and power, results are satisfactory and show a good response time and accuracy of the model.

This model can be used as a platform for simulations, comparisons and analysis of different PV-sources configurations .Moreover; it can be used to validate or diagnoses a real-time implementation.

As a future work we suggest a real time-implementation of the model or the development of this model using other software packages like Simulink, multisim or Pspice in the goals of comparisons and validations of different outputs.

[1] : Dr MALEK Ali; Contribution à la formation pour la recherche en Énergie Solaire Photovoltaïque Bulletin des Energies Renouvelables, N° 21 – 2011, CDER, Algerie.

[2]: Olivia Mah, "Fundamentals of Photovoltaic Material'', National Solar Power Research Institute, Inc 12/21/98.

[3]: Photovoltaic systems – technology fundamentals, 2004, http://www.volker-quaschning.de/articles/fundamentals3/index_e.html.

[4]: Alireza Khaligh, Omer C.Onar, 'Energy Harvesting: Solar, Wind and Ocean Energy Conversion Systems', CRC press, 2010.

[5] Mehleri, E.D., P.L. Zervas, H. Sarimveis, J.A. Palyvos, and N.C. Markatos. "Determination of the Optimal Tilt Angle and Orientation for Solar Photovoltaic Arrays."Renewable Energy 35.11 (2010): 2468-475.

[6] H. Mousazadeh et al., A review of principle and suntracking methods for maximizing solar systems output, Renewable and Sustainable Energy Reviews 13 (2009) 1800–1818.

[7] International Journal of Engineering Science and Innovative Technology (IJESIT) Volume 2, Issue 2, March 2013

[8] P. Roth et al., Cheap two axis sun following device, Energy Conversion and Management 46 (2005) 1179–1192]

Acknowledgements:

First of all, I would like to praise almighty ALLAH for giving me the power to realize this project.

I would also thank my supervisor Mr.A.Bourezg who supported me, and helped me during the different phases of the project.

Many thanks are given to all the professors and workers at the IGEE.

At last, and not least, I would like to thank Mr.Draou from the Center of research of the Renewables energies of ADRAR and the other researchers for guiding me during my project, and providing me with all the necessary needs required to realize the project.

List of figures:

List of tables:

Nomenclature:

I_{ph}: Li@?J EHJ?< F?EJE : KHH<DJ#

V_D: Di@E; < LEB8><#

V: OuJFKJ LEB8><#

I_D: Diod@: KHH<DJ#

v_{pv}: PV \EB8><#

I_{pv}: PV curHH<DJ#

I_{SH}: Short (@EK@: KHH<DJ#

$I_0$$3<L<H<;@E; <I8JKH8J@ED: KHH<DJ#

3I$4<H@I H<I@J8D: <#

3sh: Sh'KDJ H<I@J8D: <#

T_C : Actual temF<H8JKH<#

T_{Cref} : Referen@<J<C F<H8JKH<#

%&$5?<@<8E@O: EDIJ8DJ#

)+$&8D;">8F <D<H>O#

+i: Actual \@EH8;@8J@ED#

G_{ref}: RefeH<D: <@EH8;@8J@ED#

KI: S?EH": @EK@: KHH<DJ J<C F<H8JKH<: E<=@@DJ E=8: <BB#

q: T?<:?8H<E=J?<<B<: JHED#

D: L<KJO: O: B<#

T_s: T?<IM@?@D> F<H@E; #

f_s: SM@?@D> =H<GK<D: O#

T_{on}: 5?<10 J@C<@DJ?<F<H@E; #

$T_{off}$$5?<1** J@C<@DJ?<F<H@E; #

V_g: IDFKJ LEB8><E=(''(' : EDL<H<H#

i_L: T?<@D;K: JEH: KHH<DJ#

v_L: T?<@D;K: JEHLEB8><#

. $,D;K: JEHE=(''(' : EDL<H<H#

' ;' 8F8: @EHE=(' "(' : EDL<H<H#

V_0: Ou KJFKJ LEB8>< E=(' "(' : EDL<H<H#

M (D): The conversion ratio.

$L_{boundary}$: The minimum inductan< J?8J >@<I : EDJ@KEKI : ED, K: J@EDC E; <#

C_{inmin}: 5?<C @@KC : 8F8: @8D< J?8J >@<I : EDJ@KEKI : ED, K: J@EDC E; <#

V_{om}: M 8N@KC E=; : EC FED<DJ E=J?<EKJFKJ LEB8><

D_m: D?O: O B<8J C 8N@KC : EDL<H<H@FKJ FEM<H#

f: Switc?@D> =HGK<D: G#

ΔI_{Lm}: Pe8A"JE"F<8A H@FB<E=J?<@, K: JEH: KHHKDJ#

I_{om}: D(: EC FED<DJ E=J?<EKJFKJ : KHHKDJ 8J C 8N@KC EKJFKJ FEM<H#

R_{in}: The input res@J8D<#

R_{load}: The load resistance.

C_{inmin}, C_{outmin}: Input and OuJFKJ : 8F8: @EHE=(' "(' : EDL<H<H#

V_{oc}: O<D: @KK@LEB8><#

I_{sc}: Short circK@: KHHKDJ#

V_{MPP}: Voltag< 8J C 8N@KC FEM<HFE@DJ#

I_{mpp}: CKHHKDJ 8J C 8N(mum power poinJ#

K_1: CoDIJ8DJ HKB8J@D> V_{MPP} and V_{oc} .

K_2: CoDIJ8DJ HKB8J@D> V_{MPP} and I_{mpp} .

26 $2?EJELEB8@#

/ 225 $/ 8N@KC 2EM<H2E@DJ 5H8: A@D>#

2 1 $2<HJKH9 8D, 1 9I<HL<#

,D ED, $5?<,D: HC<DJ8B: ED, K: J8D<#

2,' $2<H@?<H8B,DJ<H8: <' EDJHEB<H#

1 2%/ 2$1 F<H8J@ED8B%C FB@@H#

27 / $2KB<7 @J? / E; KB8J@ED#

. ' ($. @@K@' HCIJ8B(@FB8C#